Chapter 5

How well can the observed vertical temperature changes be reconciled with our understanding of the causes of these changes?

Convening Lead Author:
Ben D. Santer

Lead Authors:
Joyce E. Penner, and Peter W. Thorne

Contributors:
W. Collins, K. Dixon, T.L. Delworth, C. Doutriaux, Chris K. Folland, Chris E. Forest, I. Held, John Lanzante, Gerald A. Meehl, V. Ramaswamy, Dian J. Seidel, M.F. Wehner, and Tom M.L. Wigley

KEY FINDINGS

PATTERN STUDIES

Fingerprint studies use rigorous statistical methods to compare spatial and temporal patterns of climate change in computer models and observations.

1. ***Both human and natural factors have affected Earth's climate. Computer models are the only tools we have for estimating the likely climate response patterns ("fingerprints") associated with different forcing mechanisms.***

To date, most formal fingerprint studies have focused on a relatively small number of climate forcings. Our best scientific understanding is that:

- Increases in well-mixed greenhouse gases (which are primarily due to fossil fuel burning) result in large-scale warming of the Earth's surface and troposphere and cooling of the stratosphere.
- Human-induced changes in the atmospheric burdens of sulfate aerosol particles cause regional-scale cooling of the surface and troposphere.
- Depletion of stratospheric ozone cools the lower stratosphere and upper troposphere.
- Large volcanic eruptions cool the surface and troposphere (over 3 to 5 years) and warm the stratosphere (over 1 to 2 years).

- Increases in solar irradiance warm throughout the atmospheric column (from the surface to the stratosphere).

2. Results from many different fingerprint studies provide consistent evidence for a human influence on the three-dimensional structure of atmospheric temperature over the second half of the 20th century.

Robust results are:

- Detection of greenhouse-gas and sulfate aerosol signals in observed surface temperature records.
- Detection of an ozone depletion signal in stratospheric temperatures.
- Detection of the combined effects of greenhouse gases, sulfate aerosols, and ozone in the vertical structure of atmospheric temperature changes (from the surface to the stratosphere).

3. Natural factors have influenced surface and atmospheric temperatures, but cannot fully explain their changes over the past 50 years.

- The multi-decadal climatic effects of volcanic eruptions and solar irradiance changes are identifiable in some fingerprint studies, but results are sensitive to analysis details.

72

73 TREND COMPARISONS

74

75 Linear trend comparisons are less powerful than "fingerprinting" for studying cause-effect
76 relationships, but can highlight important differences (and similarities) between models and
77 observations.

78

79 ***4. When run with natural and human-caused forcings, model global-mean temperature***
80 ***trends for individual atmospheric layers are consistent with observations.***

81

82 ***5. Comparing trend differences between the surface and the troposphere exposes potential***
83 ***model-data discrepancies in the tropics.***

84

85 • Differencing surface and tropospheric temperature time series (a simple measure of
86 the temperature lapse rate) removes much of the common variability between these
87 layers. This makes it easier to identify discrepancies between modeled and observed
88 lapse-rate changes.

89 • For globally-averaged temperatures, model-predicted trends in tropospheric lapse
90 rates are consistent with observed results.

91 • In the tropics, most observational datasets show more warming at the surface than in
92 the troposphere, while most model runs have larger warming aloft than at the
93 surface.

94

AMPLIFICATION OF SURFACE WARMING IN THE TROPOSPHERE

6. In the tropics, surface temperature changes are amplified in the free troposphere. Models and observations show similar amplification behavior for monthly- and interannual temperature variations, but not for decadal temperature changes.

- Tropospheric amplification of surface temperature anomalies is due to the release of latent heat by moist, rising air in regions experiencing convection.

- Despite large inter-model differences in variability and forcings, the size of this amplification effect is remarkably similar in the models considered here, even across a range of timescales (from monthly to decadal).

- On monthly and annual timescales, amplification is also a ubiquitous feature of observations, and is very similar to values obtained from models and basic theory.

- For longer-timescale temperature changes over 1979 to 1999, only one of four observed upper-air datasets has larger tropical warming aloft than in the surface records. All model runs with surface warming over this period show amplified warming aloft.

- These results have several possible explanations, which are not mutually exclusive. One explanation is that "real world" amplification effects on short and long time scales are controlled by different physical mechanisms, and models fail to capture such behavior. A second explanation is that remaining errors in some of the

observed tropospheric data sets adversely affect their long-term temperature trends. The second explanation is more likely in view of the model-to-model consistency of amplification results, the large uncertainties in observed tropospheric temperature trends, and independent physical evidence supporting substantial tropospheric warming.

OTHER FINDINGS

7. It is important to account for observational uncertainty in comparisons between modeled and observed temperature changes.

- There are large "construction uncertainties" in the process of generating climate data records from raw observations. These uncertainties can critically influence the outcome of consistency tests between models and observations.

8. Inclusion of spatially-heterogeneous forcings in the most recent climate models does not fundamentally alter simulated lapse-rate changes at the largest spatial scales.

- Changes in black carbon aerosols and land use/land cover (LULC) may have had significant influences on regional temperatures, but these influences have not been quantified in formal fingerprint studies.

- These forcings were included for the first time in about half the global model simulations considered here. Their incorporation did not significantly affect simulations of lapse-rate changes at very large spatial scales (global and tropical averages).

RECOMMENDATIONS

1. Separate the uncertainties in climate forcings from uncertainties in the climate response to forcings.

The simulations of Twentieth Century (20CEN) climate analyzed here show climate responses that differ because of differences in:

- Model physics and resolution;
- The forcings incorporated in the 20CEN experiment;
- The chosen forcing history, and the manner in which a specific forcing was applied.

We consider it a priority to partition the uncertainties in climate forcings and model responses, and thus improve our ability to interpret differences between models and observations. This could be achieved by better coordination of experimental design, particularly for the 20CEN simulations that are most relevant for direct comparison with observations.

2. Quantify the contributions of changes in black carbon aerosols and land use/land cover to recent large-scale temperature changes.

We currently lack experiments in which the effects of black carbon aerosols and LULC are varied individually (while holding other forcings constant). Such "single forcing" runs will help to quantify the contributions of these forcings to global-scale changes in lapse-rates.

3. Explicitly consider model and observational uncertainty.

Efforts to evaluate model performance or identify human-induced climate change should always account for uncertainties in both observations and in model simulations of historical and future climate. This is particularly important for comparisons involving long-term changes in upper-air temperatures. It is here that current observational uncertainties are largest and require better quantification.

4. Perform the "next generation" of detection and attribution studies.

Formal detection and attribution studies utilizing the new generation of model and observational datasets detailed herein should be undertaken as a matter of priority.

1 *Introduction*

A key scientific question addressed in this report is whether the Earth's surface has warmed more rapidly than the troposphere over the past 25 years (*NRC*, 2000). Chapter 1 noted that there are good physical reasons why we do not expect surface and tropospheric temperatures to evolve in unison at all places and on all timescales. Chapters 2, 3, and 4 summarized our current understanding of observed changes in surface and atmospheric temperatures. These chapters identified important differences between surface and tropospheric temperatures, some of which may be due to remaining problems with the observational data, and some of which are likely to be real.

In Chapter 5, we seek to explain and reconcile the apparently disparate estimates of observed changes in surface and tropospheric temperatures. We make extensive use of computer models of the climate system. In the real world, multiple "climate forcings" vary simultaneously, and it is difficult to identify and separate the climate effects of individual factors. Furthermore, the experiment that we are performing with the Earth's atmosphere lacks a suitable control – we do not have a convenient "parallel Earth" on which there are no human-induced changes in greenhouse gases, aerosols, or other climate forcings. Climate models can be used to perform such controlled experiments, or to simulate the response to changes in a single forcing or combination of forcings, and thus have real advantages for studying cause-effect relationships. However, models also have systematic errors that can diminish their usefulness as a tool for interpretation of observations (*Gates et al.*, 1999; *McAvaney et al.*, 2001).

We evaluate published research that has made rigorous quantitative comparisons of modeled and observed temperature changes, primarily over the satellite and radiosonde eras. Some new model experiments (performed in support of the IPCC Fourth Assessment Report) involve simultaneous changes in a wide range of natural and human-induced climate forcings. These experiments are highly relevant for direct comparison with satellite-, radiosonde-, and surface-based temperature observations. We review their key results here.

2 *Model Simulations of Recent Temperature Change*

Many different types of computer model are used for studying climate change issues (*Meehl*, 1984; *Trenberth*, 1992; see Box 5.1). Models span a large range of complexity, from the one- or two-dimensional energy-balance models (EBMs) through Earth System models of intermediate complexity (EMICs) to full three-dimensional atmospheric General Circulation Models (AGCMs) and coupled atmosphere-ocean GCMs (CGCMs). Each type has advantages and disadvantages for specific applications. The more complex AGCMs and CGCMs are most appropriate for understanding problems related to the atmosphere's vertical temperature structure, since they explicitly resolve that structure, and incorporate many of the physical processes (*e.g.*, convection, interactions between clouds and radiation) thought to be important in maintaining atmospheric temperature profiles. They are also capable of representing the horizontal and vertical structure of unevenly-distributed climate forcings that may contribute to differential warming of the surface and troposphere. Examples include volcanic aerosols (*Robock*, 2000) or the sulfate and soot aerosols arising from fossil fuel or biomass burning (*Penner et al.*, 2001; *Ramaswamy et al.*, 2001a,b).

BOX 5.1: Climate Models

Climate models provide us with estimates of how the real world's climate system behaves and is likely to respond to changing natural and human-caused forcings. Because of limitations in our physical understanding and computational capabilities, models are simplified and idealized representations of a very complex reality. The most sophisticated climate models are direct descendants of the computer models used for weather forecasting. While weather forecast models seek to predict the specific timing of weather events over a period of days to several weeks, climate models attempt to simulate future changes in the *average distribution* of weather events. Simulations of 21st Century climate are typically based on "scenarios" of future emissions of GHGs, aerosols and aerosol precursors, which in turn derive from scenarios of population changes, economic growth, energy usage, developments in energy production technology, *etc*.

Climate models are also used to "hindcast" the climate changes that we have observed over the 20th Century. When run in "hindcast" mode, a climate model is not constrained by *actual* weather observations from satellites or radiosondes. Instead, it is driven by our best estimates of changes in some (but probably not all) of the major "forcings", such as GHG concentrations, the Sun's energy output, and the amount of volcanic dust in the atmosphere. In "hindcast" experiments, a climate model is free to simulate the full four-dimensional (latitude, longitude, height/depth and time) distributions of temperature, moisture, *etc*. Comparing the results of such an experiment with long observational records constitutes a valuable test of model performance.

AGCM experiments typically rely on an atmospheric model driven by observed time-varying changes in sea-surface temperatures (SSTs) and sea-ice coverage. This is a standard reference experiment that many AGCMs have performed as part of the Atmospheric Model Intercomparison Project ("AMIP"; *Gates et al*., 1999). The AMIP-style experiments discussed here also include specified changes in a variety of natural and human-caused forcing factors (*Hansen et al*., 1997, 2002; *Folland et al*., 1998; *Tett and Thorne*, 2004).

In both observations and climate models, variations in the El Niño/Southern Oscillation (ENSO) have pronounced effects on surface and tropospheric temperatures (*Yulaeva and Wallace*, 1994; *Wigley*, 2000; *Santer et al*., 2001; *Hegerl and Wallace*, 2002; *Hurrell et al.*, 2003). When run in an AMIP configuration, an atmospheric model "sees" the same changes in ocean surface temperature that the real world's atmosphere experienced. The time evolution of ENSO effects on atmospheric temperature is therefore very similar in the model and observations. This facilitates the direct comparison of modeled and observed temperature changes.[1] Furthermore, AMIP experiments reduce climate noise by focusing on the random variability arising from the atmosphere rather than on the variability of the coupled atmosphere-ocean system (which is larger in amplitude). This "noise reduction" aspect of AMIP runs has been exploited in efforts to identify human effects on year-to-year changes in atmospheric temperatures (*Folland et al*., 1998; *Sexton et al*., 2001)

[1]This does not mean, however, that the atmospheric model will necessarily capture the correct amplitude and horizontal and vertical structure of the tropospheric temperature response to the specified SST ice changes. Note also that even with the specification of ocean boundary conditions, the time evolution of modes of variability that are forced by both the ocean and the atmosphere (such as the North Atlantic Oscillation; see *Rodwell et al*., 1999) will not be the same in the model and in the real world (except by chance).

[1]Volcanic forcing provides an example of the signal estimation problem. The aerosols injected into the stratosphere during a massive volcanic eruption are typically removed within 2-3 years (*Sato et al*., 1993; *Hansen et al*., 2002; *Ammann et al*., 2003). Because the large thermal inertia of the oceans cause a lag in response to this forcing, the cooling effect of the aerosols on the troposphere and surface persists for much longer than 2-3 years (*Santer et al*., 2001; *Free and Angell*, 2002; *Wigley et al*., 2005a). In the real world and in "AMIP-style" experiments, this slow, volcanically-induced cooling of the troposphere and surface is sometimes masked by the warming effects of El Niño events (*Christy and McNider*, 1994; *Wigley*, 2000; *Santer et al*., 2001), thus hampering volcanic signal estimation.

[1]There are a variety of different spin-up strategies.

[1]In most of the experiments reported on here, *n* is between 3 and 5.
and sea-ice changes. Note also that even with the specification of ocean boundary conditions, the time evolution of modes of variability that are forced by both the ocean and the atmosphere (such as the North Atlantic Oscillation; see *Rodwell et al*., 1999) will not be the same in the model and in the real world (except by chance).

One disadvantage of the AMIP experimental set-up is that significant errors in one or more of the applied forcing factors (or omission of key forcings) are not "felt" by the prescribed SSTs. Such errors are more obvious in a CGCM experiment, where the ocean surface is free to respond to imposed forcings. The lack of an ocean response and the masking effects of natural variability make it difficult to use an AMIP-style experiment to estimate the slow response of the climate system to an imposed forcing change.[2] CGCM experiments are more useful for this specific purpose (see Chapter 1, Figure 1.3).

The CGCM experiments of interest here involve a model that has been "spun-up" until it reaches some quasi-steady climate state[3]. The CGCM is then run with estimates of how a variety of natural and human-caused climate forcings have changed over the 20th century. We refer to these subsequently as "20CEN" experiments. Since the true state of the climate system is never fully known, the same forcing changes are applied *n* times,[4] each time starting from a slightly different initial climate state. This procedure yields *n* different realizations of climate change. All of these realizations contain some underlying "signal" (the climate response to the imposed forcing changes) upon which are superimposed *n* different manifestations of "noise" (natural internal climate variability). Taking averages over these *n* realizations yields less noisy estimates of the signal (*Wigley et al*., 2005a).

[2]Volcanic forcing provides an example of the signal estimation problem. The aerosols injected into the stratosphere during a massive volcanic eruption are typically removed within 2-3 years (*Sato et al*., 1993; *Hansen et al*., 2002; *Ammann et al*., 2003). Because the large thermal inertia of the oceans cause a lag in response to this forcing, the cooling effect of the aerosols on the troposphere and surface persists for much longer than 2-3 years (*Santer et al*., 2001; *Free and Angell*, 2002; *Wigley et al*., 2005a). In the real world and in "AMIP-style" experiments, this slow, volcanically-induced cooling of the troposphere and surface is sometimes masked by the warming effects of El Niño events (*Christy and McNider*, 1994; *Wigley*, 2000; *Santer et al*., 2001), thus hampering volcanic signal estimation.

[3]There are a variety of different spin-up strategies.

[4]In most of the experiments reported on here, *n* is between 3 and 5.

In a CGCM, ocean temperatures are fully predicted rather than prescribed. This means that even a (hypothetical) CGCM which perfectly captured all important aspects of ENSO physics would not have the same timing of El Niño and La Niña events as the real world (except by chance). The fact that ENSO variability – and its effects on surface and atmospheric temperatures – does not "line up in time" in observations and CGCM experiments hampers direct comparisons between the two.[5] This problem can be ameliorated by statistical removal of ENSO effects (*Santer et al*., 2001; *Hegerl and Wallace*, 2002; *Wigley et al*., 2005a).[6]

The bottom line is that AMIP-style experiments and CGCM runs are both useful tools for exploring the possible causes of differential warming.[7] We note that even if these two experimental configurations employ the same atmospheric model and the same climate forcings, they can yield noticeably different simulations of changes in atmospheric temperature profiles. These differences arise for a variety of reasons, such as AGCM-versus-CGCM differences in sea-ice coverage, SST distributions, and cloud feedbacks, and hence in climate sensitivity (*Sun and Hansen*, 2003).[8]

Most models undergo some form of "tuning". This involves changing poorly-known parameters which directly affect key physical processes, such as convection and rainfall. Parameters are varied

[5]If *n* is large enough to adequately sample the (simulated) effects of natural variability on surface and tropospheric temperatures, it is not necessarily a disadvantage that the simulated and observed variability does not line up in time. In fact, this type of experimental set-up allows one to determine whether the single realization of the observations is contained within the "envelope" of possible climate solutions that the CGCM simulates.

[6]Residual effects of these modes of variability may remain in the data.

[7]Provided that comparisons with observations account for the specific advantages and disadvantages noted above.

[8]See, for example, the Ocean A and Ocean E results in Figure 3 of *Sun and Hansen* (2003).

within plausible ranges, which are generally derived from direct observations. The aim of tuning is to reduce the size of systematic model errors and improve simulations of present-day climate. Tuning does *not* involve varying uncertain model parameters over the course of a 20CEN experiment, in order to improve a given model's simulation of observed climate change over the 20th Century.[9]

Several groups are now beginning to explore model "parameter space", and are investigating the possible impact of parameter uncertainties on simulations of mean present-day climate and future climate change (*Allen*, 1999; *Forest et al*., 2002; *Murphy et al*., 2004; *Stainforth et al*., 2005). Such work will help to quantify one component of model uncertainty. Another component of model uncertainty arises from differences in the basic structure of models.[10] Section 5 considers results from a range of state-of-the-art CGCMs, and thus samples some of the "structural uncertainty" in model simulations of 20th Century climate change (Table 5.1). A further component of the "spread" in simulations of 20th Century climate is introduced by uncertainties in the climate forcings with which models are run (Table 5.2). These are discussed in the following Section.

Table 5.1: Acronyms of climate models referenced in this Chapter. All 19 models performed simulations of 20th century climate change ("20CEN") in support of the IPCC Fourth Assessment Report. The ensemble size "ES" is the number of independent realizations of the 20CEN experiment that were analyzed here.

[9]Potentially, highly uncertain climate forcings (particularly those associated with the indirect effects of aerosol particles on clouds) could be adjusted to improve the correspondence between modeled and observed global-mean surface temperature changes over the 20th Century. Such tuning does not occur *per se* and would be an unacceptable procedure, quite different from the parameter adjustments that are made when improving AGCM and CGCM simulations of mean climate.

[10]The computer models constructed by different research groups can have quite different "structures" in terms of their horizontal and vertical resolution, atmospheric dynamics (so-called "dynamical cores"), numerical implementation (*e.g*., spectral versus grid-point), and physical parameterizations. They do, however, share many common assumptions.

	MODEL ACRONYM	COUNTRY	INSTITUTION	ES
1	CCCma-CGCM3.1(T47)	Canada	Canadian Centre for Climate Modelling and Analysis	1
2	CCSM3	United States	National Center for Atmospheric Research	5
3	CNRM-CM3	France	Météo-France/Centre National de Recherches Météorologiques	1
4	CSIRO-Mk3.0	Australia	CSIRO[1] Marine and Atmospheric Research	1
5	ECHAM5/MPI-OM	Germany	Max-Planck Institute for Meteorology	3
6	FGOALS-g1.0	China	Institute for Atmospheric Physics	1
7	GFDL-CM2.0	United States	Geophysical Fluid Dynamics Laboratory	3
8	GFDL-CM2.1	United States	Geophysical Fluid Dynamics Laboratory	3
9	GISS-AOM	United States	Goddard Institute for Space Studies	2
10	GISS-EH	United States	Goddard Institute for Space Studies	5
11	GISS-ER	United States	Goddard Institute for Space Studies	5
12	INM-CM3.0	Russia	Institute for Numerical Mathematics	1
13	IPSL-CM4	France	Institute Pierre Simon Laplace	1
14	MIROC3.2(medres)	Japan	Center for Climate System Research / NIES[2] / JAMSTEC[3]	3
15	MIROC3.2(hires)	Japan	Center for Climate System Research / NIES[2] / JAMSTEC[3]	1
16	MRI-CGCM2.3.2	Japan	Meteorological Research Institute	5
17	PCM	United States	National Center for Atmospheric Research	4
18	UKMO-HadCM3	United Kingdom	Hadley Centre for Climate Prediction and Research	1
19	UKMO-HadGEM1	United Kingdom	Hadley Centre for Climate Prediction and Research	1

[1]CSIRO is the Commonwealth Scientific and Industrial Research Organization.
[2]NIES is the National Institute for Environmental Studies.
[3]JAMSTEC is the Frontier Research Center for Global Change in Japan.

Table 5.2: Forcings used in IPCC simulations of 20th century climate change. This Table was compiled using information provided by the participating modeling centers (see http://www-pcmdi.llnl.gov/ipcc/model.documentation). Eleven different forcings are listed: well-mixed greenhouse gases (G), tropospheric and stratospheric ozone (O), sulfate aerosol direct (SD) and indirect effects (SI), black carbon (BC) and organic carbon aerosols (OC), mineral dust (MD), sea salt (SS), land use/land cover (LU), solar irradiance (SO), and volcanic aerosols (V). Shading denotes inclusion of a specific forcing. As used here, "inclusion" means specification of

a time-varying forcing, with changes on interannual and longer timescales. Forcings that were varied over the seasonal cycle only are not shaded.

	MODEL	G	O	SD	SI	BC	OC	MD	SS	LU	SO	V
1	CCCma-CGCM3.1(T47)											
2	CCSM3											
3	CNRM-CM3											
4	CSIRO-Mk3.0											
5	ECHAM5/MPI-OM											
6	FGOALS-g1.0											
7	GFDL-CM2.0											
8	GFDL-CM2.1											
9	GISS-AOM											
10	GISS-EH											
11	GISS-ER											
12	INM-CM3.0											
13	IPSL-CM4											
14	MIROC3.2(medres)											
15	MIROC3.2(hires)											
16	MRI-CGCM2.3.2											
17	PCM											
18	UKMO-HadCM3											
19	UKMO-HadGEM1											

3 *Forcings in Simulations of Recent Climate Change*

In an ideal world, there would be reliable quantitative estimates of all climate forcings – both natural and human-induced – that have made significant contributions to differential warming of the surface and troposphere. We would have detailed knowledge of spatial and temporal changes in these forcings. Finally, we would have used standard forcings to perform climate-change experiments with a whole suite of numerical models, thus isolating uncertainties arising from structural differences in the models themselves (see Box 5.2).

Box 5.2: Uncertainties in Simulated Temperature Changes

In discussing the major sources of uncertainty in observational estimates of temperature change, Chapter 2 partitioned uncertainties into three distinct categories: "structural," "parametric," and "statistical." Uncertainties in simulated temperature changes fall into similar categories. In the modeling context, "structural" uncertainties can be thought of as the uncertainties resulting from the choice of a particular climate model, model configuration (Section 2), or forcing dataset (Section 3).

Within a given model, there are small-scale physical processes (such as convection, cloud formation, precipitation, *etc*.) which cannot be simulated explicitly. Instead, so-called "parameterizations" represent the large-scale effects of these unresolved processes. Each of these has uncertainties in the values of key parameters.[11] Varying these parameters within plausible ranges introduces "parametric" uncertainty in climate change simulations (*Allen*, 1999; *Forest et al*., 2002; *Murphy et al*., 2004). Finally (analogous to the observational case), there is statistical uncertainty that arises from the unpredictable "noise" of internal climate variability, from the choice of a particular statistical metric to describe climate change, or from the application of a selected metric to noisy data.

[11]Note that some of these parameters influence not only the climate response, but also the portrayal of the forcing itself. Examples include parameters related to the size of sulfate aerosols, and how aerosol particles scatter incoming sunlight.

Unfortunately, this ideal situation does not exist. As part of the IPCC Third Assessment Report, *Ramaswamy et al*. (2001b) assigned subjective confidence levels to our current "level of scientific understanding" (LOSU) of the changes in a dozen different climate forcings. Only in the case of well-mixed greenhouse gases ("GHGs"; carbon dioxide [CO_2], methane, nitrous oxide, and halocarbons) was the LOSU characterized as "high." The LOSU of changes in stratospheric and tropospheric ozone was judged to be "medium." For all other forcings (various aerosols, mineral dust, land use-induced albedo changes, solar, *etc*.), the LOSU was estimated to be "low" or "very low" (see Chapter 1, Table 1).[12]

In selecting the forcings for simulating the climate of the 20th Century (20CEN), there are at least three strategies that modeling groups can adopt. The first strategy is to incorporate only those forcings whose changes and effects are thought to be better understood, and for which time- and space-resolved datasets suitable for performing 20CEN experiments are readily available. The second strategy is to include a large number of different forcings, even those for which the LOSU is "very low." A third strategy is to vary the size of poorly-known 20CEN forcings. This yields a range of simulated climate responses, which are then used to estimate the levels of the forcings that are consistent with observations (*e.g*., *Forest et al*., 2002).

The pragmatic focus of Chapter 5 is on climate forcings that have been incorporated in many CGCM simulations of 20th century climate. The primary forcings that we consider are changes in

[12]We note that there is no direct relationship between the LOSU of a given forcing and the contribution of that forcing to 20th Century climate change. Forcings with "low" or "very low" LOSU may have had significant climatic impacts at regional and even global scales.

well-mixed GHGs, the direct effects of sulfate aerosol particles, tropospheric and stratospheric ozone, volcanic aerosols, and solar irradiance. These are forcings whose effects on surface and atmospheric temperatures have been quantified in rigorous fingerprint studies (see Section 4). This does not diminish the importance of other climate forcings, whose global-scale contribution to "differential warming" has not been reliably quantified to date.

Examples of these "other forcings" include carbon-containing aerosols produced during fossil fuel or biomass combustion, human-induced changes in land surface properties, and the indirect effects of tropospheric aerosols on cloud properties. There is emerging scientific evidence that such spatially-variable forcings may have had important impacts on regional and even on global climate (*NRC*, 2005). Some of this evidence is summarized in Box 5.3 and Box 5.4 for the specific cases of carbonaceous aerosols and land use change. These and other previously-neglected forcings have been included in many of the new CGCM simulations of 20th century climate described in Section 5 (see Tables 5.1 and 5.2).

412 Box 5.3: Example of a Spatially-Heterogeneous Forcing: Black Carbon Aerosols
413
414 Carbon-containing aerosols (also known as "carbonaceous" aerosols) exist in a variety of chemical
415 forms (*Penner et al*., 2001). Two main classes of carbonaceous aerosol are generally distinguished:
416 "black carbon" (BC) and "organic carbon" (OC). Both types of aerosol are emitted during fossil
417 fuel and biomass burning. Most previous modeling work has focused on BC aerosols rather than
418 OC aerosols. Some of the new model experiments described in Section 5 have now incorporated
419 both types of aerosol in CGCM simulations of 20th century climate changes (see Tables 5.2 and
420 5.3).
421
422 Black carbon aerosols absorb sunlight and augment the GHG-induced warming of the troposphere
423 (*Hansen et al*., 2000; *Satheesh and Ramanathan*, 2000; *Penner et al*., 2001; *Hansen*, 2002; *Penner*
424 *et al*., 2003).[13] Their effects on atmospheric temperature profiles are complex, and depend on such
425 factors as the chemical composition, particle size, and height distribution of the aerosols (*e.g*.,
426 *Penner et al*., 2003).
427
428 *Menon et al*. (2002) showed that the inclusion of fossil fuel and biomass aerosols over China and
429 India[14] directly affected simulated vertical temperature profiles by heating the lower troposphere
430 and cooling the surface. In turn, this change in atmospheric heating influenced regional circulation
431 patterns and the hydrological cycle. *Krishnan and Ramanathan* (2002) found that an increase in
432 black carbon aerosols has reduced the surface solar insolation (exposure to sunlight) over the
433 Indian subcontinent. Model experiments performed by *Penner et al*. (2003) suggest that the net
434 effect of carbonaceous aerosols on global-scale surface temperature changes depends critically on
435 how aerosols affect the vertical distribution of clouds. On regional scales, the surface temperature
436 effects of these aerosols are complex, and vary in sign (*Penner et al*., 2005).
437

438

439

440

441

442

443

444

[13]Note that soot particles are sometimes transported long distances by winds, and can also have a "far field" effect on climate by reducing the reflectivity of snow in areas remote from pollution sources (*Hansen and Nazarenko*, 2003; *Jacobson*, 2004).

[14]During winter and spring, black carbon aerosols contribute to a persistent haze over large areas of Southern Asian and the Northern Indian Ocean (*Ramanathan et al*., 2001).

Box 5.4: Example of a Spatially-Heterogeneous Forcing: Land Use Change

Humans have transformed the surface of the planet through such activities as conversion of forest to cropland, urbanization, irrigation, and large water diversion projects (see Chapter 4). These changes can affect a variety of physical properties of the land surface, such as the albedo (reflectivity), the release of water by plants (transpiration), the moisture-holding capacity of soil, and the surface "roughness." Alterations in these physical properties may in turn affect runoff, heat and moisture exchanges between the land surface and atmospheric boundary layer, wind patterns, and even rainfall (*e.g.*, *Pitman et al*., 2004). Depending on the nature of the change, either warming or cooling of the land surface may occur (*Myhre and Myhre*, 2003).

At the regional level, modeling studies of the Florida peninsula (*Marshall et al*., 2004) and southwest Western Australia (*Pitman et al*., 2004) have linked regional-scale changes in atmospheric circulation and rainfall to human transformation of the natural vegetation. Modeling work focusing on North America suggests that the conversion of natural forest and grassland to agricultural production has led to a cooling in summertime (*Oleson et al*., 2004). The global-scale signal of land use/land cover (LULC) changes from pre-industrial times to the present is estimated to be a small net cooling of surface temperature (*Matthews et al*., 2003, 2004; *Brovkin et al*., 2004; *Hansen et al*., 2005a; *Feddema et al*., 2005). Larger regional trends of either sign are likely to be evident (*e.g.*, *Hansen et al*., 2005a).[15]

Clearly, we will *never* have complete and reliable information on all forcings that are thought to have influenced climate over the late 20th century. A key question is whether those forcings most important for understanding the differential warming problem are reliably represented. This is currently difficult to answer. What we *can* say, with some certainty, is that the expected atmospheric temperature signal due to forcing by well-mixed GHGs alone is distinctly different from the signal due to the combined effects of multiple natural and human forcing factors (Chapter 1; *Santer et al*., 1996; *Tett et al*., 1996; *Hansen et al.*, 1997, 2002; *Bengtsson et al*., 1999; *Santer et al*., 2003a).

[15]Note that larger regional trends do not necessarily translate to enhanced detectability. Although the signals of LULC and other spatially-heterogeneous forcings are likely to be larger regionally than globally, the "noise" of natural climate variability is also larger at smaller spatial scales. It is not obvious *a priori*, therefore, how signal-to-noise relationships (and detectability of a given forcing's climate effects) behave as one moves from global to continental to regional scales.

474 This is illustrated by the 20CEN and "single forcing" experiments performed with the Parallel
475 Climate Model (PCM; *Washington et al*., 2000). In PCM, changes in the vertical profile of
476 atmospheric temperature over 1979 to 1999 are primarily forced by changes in well-mixed GHGs,
477 ozone, and volcanic aerosols (Figure 5.1). Changes in solar irradiance and the scattering effects of
478 sulfate aerosols are of secondary importance over this period. Even without performing formal
479 statistical tests, it is visually obvious from Figure 5.1 that radiosonde-based estimates of observed
480 stratospheric and tropospheric temperature changes are in better agreement with the PCM 20CEN
481 experiment than with the PCM "GHG only" run.
482
483

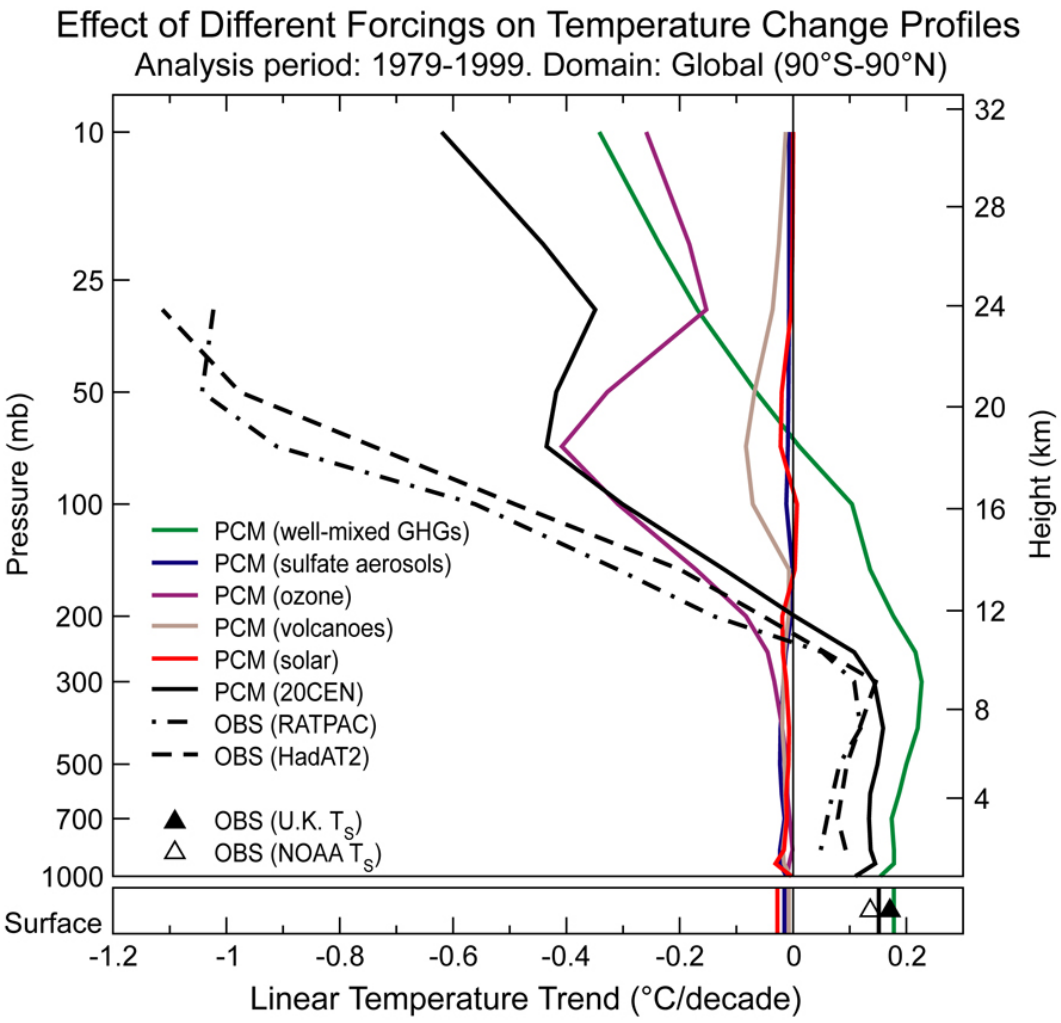

Figure 5.1: Vertical profiles of global-mean atmospheric temperature change over 1979 to 1999. Surface temperature changes are also shown. Results are from two different radiosonde data sets (HadAT2 and RATPAC; see Chapter 3) and from single forcing and combined forcing experiments performed with the Parallel Climate Model (PCM; *Washington et al*., 2000). PCM results for each forcing experiment are averages over four different realizations of that experiment. All trends were calculated with monthly mean anomaly data.

This illustrates the need for caution in comparisons of modeled and observed atmospheric temperature change. The differences evident in such comparisons have multiple interpretations. They may be due to real errors in the models,[16] errors in the forcings used to drive the models, the neglect of important forcings, and residual inhomogeneities in the observations themselves. They

[16]These may lie in the physics, parameterizations, inadequate horizontal or vertical resolution, *etc*.

may also be due to different manifestations of natural variability noise in the observations and a given CGCM realization. All of these factors may be important in model evaluation work.

4. *Published Comparisons of Modeled and Observed Temperature Changes*

A number of observational and modeling studies have attempted to shed light on the possible causes of "differential warming".[17] We have attempted to organize the discussion of results so that

[17]We do not discuss studies which provide empirical estimates of "equilibrium climate sensitivity" – the steady-state warming of the Earth's surface that would eventually be reached after the climate system equilibrated to a doubling of pre-industrial atmosp tropospheric temperatures to massive volcanic eruptions (*Hansen et al*., 1993; *Lindzen and Giannitsis*, 1998; *Douglass and Knox*, 2005; *Wigley et al*., 2005a,b; *Robock*, 2005); the "intermediate" (100- to 150-year) response of surface temperatures to natural and human-caused forcing changes over the 19th and 20th centuries (*Andronova and Schlesinger*, 2001; *Forest et al*., 2002; *Gregory et al*., 2002; *Harvey and Kaufmann*, 2002) or to solar and volcanic forcing changes over the past 1-2 millennia (*Crowley*, 2000), and the slow (100,000-year) response of Earth's temperature to orbital changes between glacial and interglacial conditions (*Hoffert and Covey*, 1992; *Hansen et al*., 1993). These investigations are not directly relevant to elucidation of the causes of changes in the vertical structure of atmospheric temperatures, which is the focus of our Chapter.

[17]It is useful to mention one technical issue relevant to model-data comparisons. As noted in Chapter 2, the satellite-based Microwave Sounding Unit (MSU) monitors the temperature of very broad atmospheric layers. To facilitate comparisons with observed MSU datasets, many of the studies reported on here calculate "synthetic" MSU temperatures from climate model experiments. Technical aspects of these calculations are discussed in Chapter 2, Box 2.

[17]The studies by *Jones* (1994) and *Christy and McNider* (1994) remove volcano and ENSO effects from T_{2LT}, and estimate residual trends of 0.093 and 0.090°C/decade over 1979 to 1993. A similar investigation by *Michaels and Knappenberger* (2000) obtained a residual trend of 0.041°C/decade over 1979 to 1999. The error bars on these residual trend estimates are either not given, or claimed to be very small (*e.g*., ± 0.005°C/decade in *Christy and McNider*). A fourth study removed combined ENSO, volcano, and solar effects from T_{2LT}, and estimated a residual trend of 0.065 ± 0.012°C/decade over 1979 to 2000 (*Douglass and Clader*, 2000).
heric CO_2 levels. This is often referred to as $\Delta T_{2\times CO2}$. Estimates of $\Delta T_{2\times CO2}$ have been obtained by studying Earth's temperature response to "fast", "intermediate", and "slow" forcing of the climate system. Examples include the "fast" (<10-year) response of surface and tropospheric temperatures to massive volcanic eruptions (*Hansen et al*., 1993; *Lindzen and Giannitsis*, 1998; *Douglass and Knox*, 2005; *Wigley et al*., 2005a,b; *Robock*, 2005); the "intermediate" (100- to 150-year) response of surface temperatures to natural and human-caused forcing changes over the 19th and 20th centuries (*Andronova and Schlesinger*, 2001; *Forest et al*., 2002; *Gregory et al*., 2002; *Harvey and Kaufmann*, 2002) or to solar and volcanic forcing changes over the past 1-2 millennia (*Crowley*, 2000), and the slow (100,000-year) response of Earth's temperature to orbital changes between glacial and interglacial conditions (*Hoffert and Covey*, 1992; *Hansen et al*., 1993). These investigations are not directly relevant to elucidation of the causes of changes in the vertical structure of atmospheric temperatures, which is the focus of our Chapter.

investigations with similar analysis methods are grouped together.[18] Our discussion proceeds from simple to more complex and statistically rigorous analyses.

4.1 *Regression studies using observed global-mean temperature data*

One class of study that has attempted to address the causes of recent tropospheric temperature change relies on global-mean observational data only (*Jones*, 1994; *Christy and McNider*, 1994; *Michaels and Knappenberger*, 2000; *Douglass and Clader*, 2002). Such work uses a multiple regression model to quantify the statistical relationships between various "predictor variables" (typically time series of ENSO variability, volcanic aerosol loadings, and solar irradiance) and a single "predictand" (typically T_{2LT}). The aim is to remove the effects of the selected predictors on tropospheric temperature, and to estimate the residual trend that may arise from human-induced forcings. The quoted values for this residual trend in T_{2LT} range from 0.04 to 0.09°C/decade.[19]

These studies make the unrealistic assumption that the uncertainties inherent in such statistical signal separation exercises are very small. They do not explore the sensitivity of regression results to uncertainties in the predictor variables, and generally use solar and volcanic *forcings* as predictors rather than the climate *responses* to those forcings. Distinctions between forcing and

[18]It is useful to mention one technical issue relevant to model-data comparisons. As noted in Chapter 2, the satellite-based Microwave Sounding Unit (MSU) monitors the temperature of very broad atmospheric layers. To facilitate comparisons with observed MSU datasets, many of the studies reported on here calculate "synthetic" MSU temperatures from climate model experiments. Technical aspects of these calculations are discussed in Chapter 2, Box 2.

[19]The studies by *Jones* (1994) and *Christy and McNider* (1994) remove volcano and ENSO effects from T_{2LT}, and estimate residual trends of 0.093 and 0.090°C/decade over 1979 to 1993. A similar investigation by *Michaels and Knappenberger* (2000) obtained a residual trend of 0.041°C/decade over 1979 to 1999. The error bars on these residual trend estimates are either not given, or claimed to be very small (*e.g.*, ± 0.005°C/decade in *Christy and McNider*). A fourth study removed combined ENSO, volcano, and solar effects from T_{2LT}, and estimated a residual trend of 0.065 ± 0.012°C/decade over 1979 to 2000 (*Douglass and Clader*, 2000).

520 response are important (*Wigley et al*., 2005a). Accounting for uncertainties in predictor variables
521 (and use of responses rather than forcings as predictors) expands the range of uncertainties in
522 estimates of residual T_{2LT} trends (*Santer et al*., 2001).[20]
523
524 Regression methods have also been used to estimate the net effects of ENSO and volcanoes on
525 trends in global-mean surface and tropospheric temperatures. For T_{2LT}, both *Jones* (1994) and
526 *Christy and McNider* (1994) found that ENSO effects induced a small net warming of 0.03 to
527 0.05°C/decade over 1979 to 1993, while volcanoes caused a cooling of 0.18°C/decade over the
528 same period. *Michaels and Knappenberger* (2000) also reported a relatively small ENSO influence
529 on T_{2LT} trends.[21] *Santer et al*. (2001) noted that over 1979 to 1997, volcanoes had likely cooled the
530 troposphere by more than the surface. Removing the combined volcano and ENSO effects from
531 surface and UAH T_{2LT} data helped to explain some of the observed differential warming: the "raw"
532 T_S-minus-T_{2LT} trend over 1979 to 1997 decreased from roughly 0.15°C/decade to 0.05°-
533 0.13°C/decade.[22] Removal of volcano and ENSO influences also brought observed lapse rate trends
534 closer to model results, but could not fully reconcile modeled and observed lapse rate trends.[23]
535

[20]*Santer et al*. (2001) obtain residual T_{2LT} trends ranging from 0.06 to 0.16°C/decade over 1979 to 1999. Their regression model is iterative, and involves removal of ENSO and volcano effects only.

[21]Their T_{2LT} trends were 0.04°C/decade over 1979 to 1998 and 0.01°C/decade over 1979 to 1999. This difference in the net ENSO influence on T_{2LT} (with the addition of only a single year of record) arises from the El Niño event in 1997/98, and illustrates the sensitivity of this kind of analysis to so-called "end effects".

[22]The latter results were obtained with the HadCRUTv surface data (*Jones et al*., 2001) and version d03 of the UAH T_{2LT} data. The range of residual lapse-rate trends arises from parametric uncertainty, *i.e*., from the different choices of ENSO predictor variable and volcano parameters.

[23]*Santer et al*. (2001) analyzed model experiments performed with the ECHAM4/OPYC model developed at the Max-Planck Institute for Meteorology in Hamburg (*Roeckner et al*., 1999). The experiments included forcing by well-mixed greenhouse gases, direct and indirect sulfate aerosol effects, tropospheric and stratospheric ozone, and volcanic aerosols (Pinatubo only).

4.2 *Regression studies using spatially-resolved temperature data*

Other regression studies have attempted to remove natural variability influences using spatially-resolved temperature data. Regression is performed "locally" at individual grid-points and/or atmospheric levels. To obtain a clearer picture of volcanic effects on atmospheric temperatures, *Free and Angell* (2002) removed the effects of variability in ENSO and the Quasi-Biennial Oscillation (QBO) from Hadley Centre radiosonde data[24]. Their work clearly shows that the cooling effect of massive volcanic eruptions has been larger in the upper troposphere than in the lower troposphere. The implication is that volcanic effects probably contribute to slow changes in observed lapse rates.

Hegerl and Wallace (2002) used regression methods to identify and remove different components of natural climate variability from gridded fields of surface temperature data, the UAH T_{2LT}, and "synthetic" T_{2LT} calculated from radiosonde data. They focused on the variability associated with ENSO and the so-called "cold ocean warm land" (COWL) pattern (*Wallace et al*., 1995). While ENSO and COWL variability made significant contributions to the month-to-month and year-to-year variability of temperature differences between the surface and T_{2LT}, it had very little impact on decadal fluctuations in lapse rate. The authors concluded that natural variability alone was unlikely to explain these slow lapse-rate changes. However, the removal of ENSO and COWL effects more clearly revealed a volcanic contribution, consistent with the findings of *Santer et al*. (2001) and

[24]The HadRT2.1 dataset of Parker *et al*. (1997). Like *Santer et al.* (2001), *Free and Angell* (2002) also found some sensitivity of the estimated volcanic signals to "parametric" uncertainty.

Free and Angell (2002). A climate model control run (with no changes in forcings) and a 20CEN experiment were unable to replicate the observed decadal changes in lapse rate.[25]

4.3 *Other studies of global and tropical lapse-rate trends*

Several studies have investigated lapse-rate trends without attempting to remove volcano effects or natural climate noise. *Brown et al*. (2000) used surface, radiosonde, and satellite data to identify slow, tropic-wide changes in the lower tropospheric lapse rate.[26] In their analysis, the surface warmed relative to the troposphere between the early 1960s and mid-1970s and after the early 1990s. Between these two periods, the tropical troposphere warmed relative to the surface. The spatial coherence of these variations (and independent evidence of concurrent variations in the tropical general circulation) led *Brown et al*. (2000) to conclude that tropical lapse rate changes were unlikely to be an artifact of residual errors in the observations.

Very similar decadal changes in lower tropospheric lapse rate were reported by *Gaffen et al*. (2000).[27] Their study analyzed radiosonde-derived temperature and lapse rate changes over two periods: 1960 to 1997 and 1979 to 1997. Tropical lapse rates decreased over the longer period[28]

[25]The model was the ECHAM4/OPYC CGCM used by *Bengtsson et al*. (1999). The 20CEN experiment analyzed by *Hegerl and Wallace* (2002) involved combined changes in well-mixed greenhouse gases, the direct and indirect effects of sulfate aerosols, and tropospheric ozone. Forcing by volcanoes and stratospheric ozone depletion was not included.

[26]The *Brown et al*. (2000) study employed UKMO surface data (HadCRUT), version d of the UAH T_{2LT}, and an early version of the Hadley Centre radiosonde dataset (HadRT2.0) that was uncorrected for instrumental biases.

[27]*Gaffen et al*. (2000) used a different radiosonde dataset from that employed by *Brown et al*. (2000). The two groups also analyzed different surface temperature datasets.

[28]Corresponding to a tendency towards a more stable atmosphere.

573 and increased over the satellite era.[29] To evaluate whether natural climate variability could explain
574 these slow variations, *Gaffen et al*. (2000) computed lapse rates from the control runs performed
575 with three different CGCMs. Each control run was 300 years in length. These long runs provided
576 estimates of the "sampling variability" of modeled lapse rate changes on timescales relevant to the
577 two observational periods (38 and 19 years).[30] Model-based estimates of natural climate variability
578 could not explain the observed tropical lapse rate changes over 1979 to 1997. Similar conclusions
579 were reached by *Hansen et al*. (1995) and *Santer et al*. (2000). Including natural and anthropogenic
580 forcings in the latter study narrowed the gap between modeled and observed estimates of recent
581 lapse-rate changes, although a significant discrepancy between the two still remained.
582
583 It should be emphasized that *all* of the studies reported on to date in Section 4 relied on satellite
584 data from one group only (UAH), on early versions of the radiosonde data[31], and on experiments
585 performed with earlier model "vintages." It is likely, therefore, that this work may have
586 underestimated the structural uncertainties in observed and simulated estimates of lapse rate
587 changes. We will consider in Section 5 whether modeled and observed lapse rate changes can be
588 better reconciled by the availability of more recent 20CEN runs and more comprehensive estimates
589 of structural uncertainties in observations.
590

[29]These lapse-rate changes were accompanied by increases and decreases in tropical freezing heights (which were inferred from the same radiosonde data).

[30]This was done by generating, for each control run, distributions of 38-year and 19-year lapse rate trends. For example, a 300-year control run can be split up into 15 different "segments" that are each of length 19 years (assuming there is no overlap between segments). From these segments, one obtains 15 different estimates of how the lapse rate might vary in the absence of any forcing changes. The observed lapse rate change over 1979 to 1997 is then compared with the model trend distribution to determine whether the observed result could be explained by natural variability alone.

[31]These radiosonde datasets were either unadjusted for inhomogeneities, or had not been subjected to the rigorous adjustment procedures used in more recent work (*Lanzante et al*., 2003; *Thorne et al*., 2005).

591 4.4 *Pattern-based "fingerprint" detection studies*

592

593 Fingerprint detection studies rely on *patterns* of temperature change (Box 5.5). The patterns are
594 typically either latitude-longitude "maps" (*e.g.*, for T_4, T_2, T_S, *etc.*) or latitude-height cross-sections
595 through the atmosphere.[32] The basic premise in fingerprinting is that different climate forcings have
596 different characteristic patterns of temperature response ("fingerprints"), particularly in the free
597 atmosphere (Chapter 1, Figure 1.3; *Hansen et al.*, 1997, 2002, 2005a; *Bengtsson et al.*, 1999;
598 *Santer et al.*, 1996; *Tett et al.*, 1996).

599

600

601

602

603

604

605

606

607

608

609

610

611

[32]In constructing these cross-sections, the temperature changes are generally averaged along individual bands of latitude. Zonal averages are then displayed at individual pressure levels, starting at the lowest model or radiosonde level and ending at the top of the model atmosphere or highest reported radiosonde level (see, *e.g.*, Chapter 1, Figure 3).

Box 5.5: Fingerprint Studies

Detection and attribution ("D&A") studies attempt to represent an observed climate dataset as a linear combination of the climate signals ("fingerprints") arising from different forcing factors and the noise of natural internal climate variability (Section 4.4). A number of different fingerprint methods have been applied to the problem of identifying human-induced climate change. Initial studies used relatively simple pattern correlation methods (*Barnett and Schlesinger, 1987; Santer et al*., 1996; *Tett et al*., 1996). Later work involved variants of the "optimal detection" approach suggested by *Hasselmann* (1979, 1993, 1997).[33] These are essentially regression-based techniques that seek to estimate the strength of a given fingerprint pattern in observational data (*i.e*., how much a given fingerprint pattern has to be scaled up or down in order to best match observations). For example, if the regression coefficient for a GHG-induced T_S fingerprint is significantly different from zero, GHG effects are deemed to be "detected" in observed surface temperature records. Attribution tests address the question of whether these regression coefficients are also consistent with unity – in other words, whether the size of the model fingerprint is consistent with its amplitude in observations (*e.g*., *Allen and Tett*, 1999; *Mitchell et al*., 2001).

There are two broad classes of regression-based D&A methods (*Mitchell et al*., 2001). One class assumes that although the fingerprint's amplitude changes over time, its spatial pattern does not (*Hegerl et al*., 1996, 1997; *Santer et al*., 2003a,b, 2004). The second class explicitly considers both the spatial structure and time evolution of the fingerprint (*Allen and Tett*, 1999; *Allen et al*., 2005; *Stott and Tett*, 1998; *Stott et al*., 2000; *Tett et al*., 1999, 2002; *Barnett et al*., 2001, 2005). This is particularly useful if the time evolution of the fingerprint contains specific information (such as a periodic 11-year solar cycle) that may help to distinguish it from natural internal climate variability (*North et al*., 1995; *North and Stevens*, 1998).

A number of choices must be made in applying D&A methods to real-world problems. One of the most important decisions relates to "reduction of dimensionality". D&A methods require some knowledge of the correlation structure of natural climate variability.[34] This structure is difficult to estimate reliably, even from long model control runs, because the number of time samples available to estimate correlation behavior is typically much smaller than the number of spatial points in the field. In practice, the total amount of spatial information (the "dimensionality") must be reduced. This is often done by using a mathematical tool (Empirical Orthogonal Functions) to reduce a complex space-time dataset to a very small number of spatial patterns ("EOFs") that capture most of the information content of the dataset.[35] Different analysts use different procedures to determine the number of patterns to retain. Further decisions relate to the choice of data used for estimating

[33] *Hasselmann* (1979) noted that the engineering field had extensive familiarity with the problem of identifying coherent signals embedded in noisy data, and that many of the techniques routinely used in signal processing were transferable to the problem of detecting a human-induced climate change signal.

[34] The relationship between variability at different points in a spatial field.

[35] The number of patterns retained is often referred to as the "truncation dimension". How the truncation dimension should be determined is a key decision in optimal detection studies (*Hegerl et al*., 1996; *Allen and Tett*, 1999).

fingerprint and noise, the number of fingerprints considered, the selection of observational data, the treatment of missing data, *etc*.[36]

D&A methods have some limitations. They do not work well if fingerprints are highly uncertain, or if the fingerprints arising from two different forcings are similar.[37] They make at least two important assumptions: that model-based estimates of natural climate variability are a reliable representation of "real-world" variability, and that the sum of climate responses to individual forcing mechanisms is equivalent to the response obtained when these factors are varied in concert. Testing the validity of both assumptions remains an important research activity (*Allen and Tett*, 1999; *Santer et al*., 2003a; *Gillett et al*., 2004a).

Most analysts rely on a climate model to provide physically-based estimates of each fingerprint's structure, size, and evolution. The model fingerprints are searched for in observational climate records, using rigorous statistical methods to quantify the degree of correspondence with observed patterns of climate change.[38] Fingerprints are also compared with patterns of climate change in model control runs. This helps to determine whether the correspondence between the fingerprint and observations is truly significant, or could arise through internal variability alone (Box 5.5). Model errors in internal variability[39] can bias detection results, although most detection work tries to guard against this possibility by performing "consistency checks" on modeled and observed variability (*Allen and Tett*, 1999), and by using variability estimates from multiple models (*Hegerl et al*., 1997; *Santer et al*., 2003a,b).

[36]Another important choice determines whether global-mean changes are included or removed from the detection analysis. Removal of global means focuses attention on smaller-scale features of modeled and observed climate-change patterns, and provides a more stringent test of model performance.

[37]This problem is known as "degeneracy". Formal tests of fingerprint degeneracy are sometimes applied (*e.g*., *Tett et al*., 2002).

[38]The fingerprint can be either the response to an individual forcing or a combination of forcings. One strategy, for example, is to search for the climate fingerprint in response to combined changes in a suite of different human-caused forcings.

[39]For example, current CGCMs fail to simulate the stratospheric temperature variability associated with the QBO or with solar-induced changes in stratospheric ozone (*Haigh*, 1994). Such errors may help to explain why one particular CGCM underestimated observed temperature variability in the equatorial stratosphere (*Gillett*, 2000). In the same model, however, the variability of temperatures and lapse rates in the tropical troposphere was in reasonable agreement with observations.

668

669 The application of fingerprint methods involves a variety of decisions, which introduce uncertainty
670 in detection results (Box 5.5). Our confidence in fingerprint detection results is increased if they are
671 shown to be consistent across a range of plausible choices of statistical method, processing options,
672 and model and observational datasets.

673

674 *Surface temperature changes*

675

676 Most fingerprint detection studies have focused on surface temperature changes. The common
677 denominator in this work is that the model fingerprints resulting from forcing by well-mixed GHGs
678 and sulfate aerosols[40] are statistically identifiable in observed surface temperature records (*Hegerl*
679 *et al*., 1996, 1997; *North and Stevens*, 1998; *Tett et al*., 1999, 2002; *Stott et al*., 2000). These results
680 are robust to a wide range of uncertainties (*Allen et al*., 2005).[41] In summarizing this body of work,
681 the IPCC concluded that "There is new and stronger evidence that most of the warming observed
682 over the last 50 years is attributable to human activities" (*Houghton et al*., 2001, page 4). The
683 causes of surface temperature change over the first half of the 20th Century are more ambiguous
684 (*IDAG*, 2005).

685

686 Most of the early fingerprint detection work dealt with global-scale patterns of surface temperature
687 change. The positive detection results obtained for "GHG-only" fingerprints were driven by model-

[40]Most of this work considers only the direct scattering effects of sulfate aerosols on incoming sunlight, and not indirect aerosol effects on clouds.

[41]For example, to uncertainties in the applied greenhouse-gas and sulfate aerosol forcings, the model responses to those forcings, and model-based estimates of natural internal climate variability.

688 data pattern similarities at very large spatial scales (*e.g.*, at the scale of individual hemispheres, or
689 land-versus-ocean behavior). Fingerprint detection of GHG effects becomes more challenging at
690 continental or sub-continental scales.[42] It is at these smaller scales that spatially heterogeneous
691 forcings, such as those arising from changes in aerosol loadings and land use patterns, may have
692 large impacts on regional climate (see Box 5.3 and 5.4). This is illustrated by the work of *Stott and*
693 *Tett* (1998), who found that a combined GHG and sulfate aerosol signal was identifiable at smaller
694 spatial scales than a "GHG-only" signal.
695
696 Recently, *Stott* (2003) and *Zwiers and Zhang* (2003) have claimed positive identification of the
697 continental- or even sub-continental features of combined GHG and sulfate aerosol fingerprints in
698 observed surface temperature records.[43] Using a variant of "classical" fingerprint methods,[44] *Min et*
699 *al*. (2005) identified a GHG signal in observed records of surface temperature change over East
700 Asia. *Karoly and Wu* (2005) suggest that GHG and sulfate aerosol effects are identifiable at even
701 smaller spatial scales ("of order 500 km in many regions of the globe"). These preliminary
702 investigations raise the intriguing possibility of formal detection of anthropogenic effects at
703 regional scales that are of direct relevance to policymakers.
704
705 *Changes in latitude/longitude patterns of atmospheric temperature or lapse rate*
706

[42]This is partly due to the fact that natural climate noise is larger (and models are less skillful) on smaller spatial scales.

[43]Another relevant "sub-global" detection study is that by *Karoly et al*. (2003). This showed that observed trends in a variety of area-averaged "indices" of North American climate (*e.g.*, surface temperature, daily temperature range, and the amplitude of the seasonal cycle) were consistent with model-predicted trends in response to anthropogenic forcing, but were inconsistent with model estimates of natural climate variability.

[44]Involving Bayesian statistics.

Fingerprint methods have also been applied to spatial "maps" of changes in layer-averaged atmospheric temperatures (*Santer et al*., 2003b; *Thorne et al*., 2003) and lapse rate (*Thorne et al*., 2003). The study by *Santer et al*. (2003b) compared modeled and observed changes in T_2 and T_4. Model fingerprints were estimated from 20CEN experiments performed with PCM (see Table 5.1), while observations were taken from two different satellite datasets (UAH and RSS; see *Christy et al*., 2003, and *Mears et al.,* 2003). The aim of this work was to assess the sensitivity of detection results to structural uncertainties in observed MSU data.

For the T_4 layer, the model fingerprint of combined human and natural effects was consistently detectable in both satellite datasets. In contrast, PCM's T_2 fingerprint was identifiable in RSS data (which show net warming over the satellite era), but not in UAH data (which show little overall change in T_2; see Chapter 3). Encouragingly, once the global-mean differences between RSS and UAH data were removed, the PCM T_2 fingerprint was detectable in *both* observed datasets. This suggests that the structural uncertainties in RSS and UAH T_2 data are most prominent at the global-mean level, and that this global-mean difference masks underlying similarities in smaller-scale pattern structure (Chapter 4; *Santer et al*., 2004).

Thorne et al. (2003) applied a "space-time" fingerprint method to six individual climate variables. These variables contained information on patterns[45] of temperature change at the surface, in broad atmospheric layers (the upper and lower troposphere), and in the lapse rates between these layers.[46]

[45]The "patterns" are in the form of temperature averages calculated over large areas rather than temperatures on a regular latitude/longitude grid.

[46]*Thorne et al*. calculated the lapse rate changes between the surface and lower troposphere, the surface and upper troposphere, and the lower and upper troposphere.

Thorne et al. explicitly considered uncertainties in the searched-for fingerprints, the observed radiosonde data[47], and in various data processing/fingerprinting options. They also assessed the detectability of fingerprints arising from multiple forcings.[48] The "bottom-line" conclusion of *Thorne et al*. is that two human-caused fingerprints – one arising from changes in well-mixed GHGs alone, and the other due to combined GHG and sulfate aerosol effects – were robustly identifiable in the observed surface, lower tropospheric, and upper tropospheric temperatures. Evidence for the existence of a detectable volcanic signal was more equivocal. Volcanic and human-caused fingerprints were not consistently identifiable in observed patterns of lapse rate change.[49]

Changes in latitude/height profiles of atmospheric temperature

Initial detection work with zonal-mean profiles of atmospheric temperature change used pattern correlations to compare model fingerprints with radiosonde data (*Karoly et al*., 1994; *Santer et al*., 1996; *Tett et al*., 1996; *Folland et al*., 1998; *Sexton et al*., 2001). These early investigations found that model fingerprints of the stratospheric cooling and tropospheric warming in response to increases in atmospheric CO_2 were identifiable in observations (Chapter 1, Figure 1.3a). The pattern similarity between modeled and observed changes generally increased over the period of the radiosonde record.

[47]The model fingerprint was estimated from 20CEN runs performed with two different versions of the Hadley Centre CGCM (HadCM2 and HadCM3). Observational data were taken from two early compilations of the Hadley Centre radiosonde data (HadRT2.1 and HadRT2.1s).

[48]Well-mixed greenhouse gases, the direct effects of sulfate aerosols, combined greenhouse-gas and sulfate aerosol effects, volcanic aerosols, and solar irradiance changes.

[49]The failure to detect volcanic signals is probably due to the coarse time resolution of the input data (five-year averages) and the masking effects of ENSO variability in the radiosonde observations. Note that the two models employed in this work yielded different estimates of the size of the natural and human-caused fingerprints.

746

747 The inclusion of other human-induced forcings in 20CEN experiments – particularly the effects of
748 stratospheric ozone depletion and sulfate aerosols – tended to improve agreement with observations
749 (*Santer et al*., 1996a; *Tett et al*., 1996; *Sexton et al*., 2001). The addition of ozone depletion cooled
750 the lower stratosphere and upper troposphere. This brought the height of the "transition level"
751 between stratospheric cooling and tropospheric warming lower down in the atmosphere, and in
752 better accord with observations (Chapter 1, Figure 1.3F). It also improved the agreement between
753 simulated and observed patterns of T_4 (*Ramaswamy et al*., 1996), and decreased the size of the
754 "warming maximum" in the upper tropical troposphere, a prominent feature of CO_2-only
755 experiments (compare Figures 1.3A and 1.3F in Chapter 1).

756

757 Early work on the direct scattering effects of sulfate aerosols suggested that this forcing was
758 generally stronger in the Northern Hemisphere (NH) than in the Southern Hemisphere (SH), due to
759 the larger emissions of sulfur dioxide in industrialized regions of the NH. This asymmetry in the
760 distribution of anthropogenic sulfur dioxide sources should yield greater aerosol-induced
761 tropospheric cooling in the NH (*Santer et al*., 1996a,b). Other forcings can lead to different
762 hemispheric temperature responses. Increases in atmospheric CO_2, for example, tend to warm land
763 more rapidly than ocean (Chapter 1). Since there is more land in the NH than in the SH, the
764 expected signal due to CO_2 increases is greater *warming* in the NH than in the SH. Because the
765 relative importance of CO_2 and sulfate aerosol forcings evolves in a complex way over time (*Tett et*
766 *al*., 2002; *Hansen et al*., 2002),[50] the "imprints" of these two forcings on NH and SH temperatures
767 must also vary with time (*Santer et al*., 1996b; Stott *et al*., 2005).

768

[50]See, for example, Figure 1a in *Tett et al*. (2002) and Figure 8b in *Hansen et al*. (2002).

769 Initial attempts to detect sulfate aerosol effects on atmospheric temperatures did not account for
770 such slow changes in the hemispheric-scale features of the aerosol fingerprint. They searched for a
771 *time-invariant* fingerprint pattern in observed radiosonde data (*Santer et al*., 1996a). This yielded
772 periods of agreement and periods of disagreement between the (fixed) aerosol fingerprint and the
773 time-varying effect of aerosols on atmospheric temperatures. Some have interpreted the periods of
774 disagreement as 'evidence of absence' of a sulfate aerosol signal (*Michaels and Knappenberger*,
775 1996). However, subsequent studies (see below) illustrate that such behavior is expected if one uses
776 a fixed sulfate aerosol fingerprint, and that it is important for detection studies to account for large
777 temporal changes in the fingerprint.
778
779 "Space-time" optimal detection schemes explicitly account for time variations in the signal pattern
780 and in observational data (Box 5.5). Results from recent "space-time" detection studies support
781 previous claims of an identifiable sulfate aerosol effect on surface temperature (*Stott et al*., 2005)
782 and on zonal-mean profiles of atmospheric temperature (*Allen and Tett*, 1999; *Forest et al*., 2001,
783 2002; *Thorne et al*., 2002; *Tett et al*., 2002; *Jones et al*., 2003). This work also illustrates that the
784 identification of human effects on atmospheric temperatures can be achieved using tropospheric
785 temperatures alone (*Thorne et al*., 2002). Positive detection results are not solely driven by the
786 inclusion of strong stratospheric cooling in the vertical pattern of temperature change (as has been
787 claimed by *Weber*, 1996).
788
789 In summary, fingerprint detection studies provide strong and consistent evidence that human-
790 induced changes in greenhouse gases and sulfate aerosols are identifiable in radiosonde records of
791 free atmospheric temperature change. The fingerprint evidence is much more equivocal in the case

792 of solar and volcanic signals in the troposphere. These natural signals have been detected in some
793 studies (*Jones et al*., 2003) but not in others (*Tett et al*. 2002), and their identification appears to be
794 more sensitive to specific processing choices that are made in applying fingerprint methods (*Leroy*,
795 1998; *Thorne et al*., 2002, 2003).
796
797 ## 5 *New Comparisons of Modeled and Observed Temperature Changes*
798
799 In this section, we evaluate selected results from recently-completed CGCM 20CEN experiments
800 that have been performed in support of the IPCC Fourth Assessment Report (AR4). The runs
801 analyzed here were performed with 19 different models, and involve modeling groups in 10
802 different countries (Table 5.1). They use new model versions, and incorporate historical changes in
803 many (but not all) of the natural and human forcings that are thought to have influenced
804 atmospheric temperatures over the past 50 years[51] (Table 5.2). These new experiments provide our
805 current best estimates of the expected climate change due to combined human and natural effects.
806
807
808
809 The new 20CEN runs constitute an "ensemble of opportunity" (*Allen and Stainforth*, 2002). The
810 selection and application of natural and anthropogenic forcings was not coordinated across
811 modeling groups.[52] For example, only seven of the 19 modeling groups applied time-varying

[51]This was not the case in previous model intercomparison exercises, such as AMIP (*Gates et al*., 1999) and CMIP2 (*Meehl et al*., 2000).

[52]In practice, experimental coordination is very difficult across a range of models of varying complexity and sophistication. Aerosols are a case in point. Some modeling groups that contributed 20CEN simulations to the IPCC AR4 do not have the technical capability to explicitly include aerosols, and instead attempt to represent their net radiative effects by adjusting the surface albedo.

812 changes in LULC (Table 5.2). Groups that included LULC effects did not always use the same
813 observational dataset for specifying this forcing, or apply it in the same way (Table 5.3). Only six
814 models included some representation of the indirect effects of anthropogenic aerosols, which are
815 thought to have had a net cooling influence on surface temperatures through their effects on cloud
816 properties (*Ramaswamy et al*., 2001b).
817
818
819
820
821
822
823
824
825
826
827
828

829 Table 5.3: Forcings used in 20CEN experiments performed with the PCM, CCSM3.0, GFDL CM2.1, and GISS-EH
830 models. Grey shading denotes a forcing that was included in the experimental design. Shading indicates a forcing that
831 was not incorporated or that did not vary over the course of the experiment.

	PCM	CCSM3.0	GFDL CM2.1	GISS-EH
Well-mixed greenhouse gases	IPCC Third Assessment Report.	IPCC Third Assessment Report.	IPCC Third Assessment Report and *World Meteorological Organization* (2003).	CH_4, N_2O and CFC spatial distributions are fit to *Minschwaner et al*. (1998).
Sulfate aerosols (direct effects)	Spatial patterns of sulfur dioxide [SO_2] emissions prescribed over seasonal cycle. Year-to-year changes scaled by estimates of historical changes in SO_2 emissions.[1]	Sulfur cycle model using time and space-varying SO_2 emissions (*Smith et al*., 2001, 2005).[2]	Computed from an atmospheric chemistry transport model.[3]	Based on simulations of *Koch et al*. (1999) and *Koch* (2001).[4]
Sulfate aerosols (indirect effects)	Not included.	Not included.	Not included.	Parameterization of aerosol indirect effects on cloud albedo and cloud cover.[4]
Stratospheric ozone	Assumed to be constant up to 1970. After 1970 prescribed from a NOAA dataset.[1]	Assumed to be constant up to 1970. After 1970 prescribed from a NOAA dataset.[2]	Specified using data from *Randel and Wu* (1999).	Specified using data from *Randel and Wu* (1999).[4]
Tropospheric ozone	Computed from an atmospheric chemistry transport model. Held constant after 1990.[1]	Computed from an atmospheric chemistry transport model. Held constant after 1990.[2]	Computed from an atmospheric chemistry transport model.[3]	Computed from an atmospheric chemistry transport model (*Shindell et al*., 2003).[4]
Black carbon aerosols	Not included.	Present-day estimate of distribution and amount of black carbon, scaled by population changes over 20th Century.[2]	Computed from an atmospheric chemistry transport model.[3]	Based on simulations of *Koch et al*. (1999) and *Koch* (2001).[4]
Organic aerosols	Not included.	Not included.	Computed from an atmospheric chemistry transport model.[3]	Based on simulations of *Koch et al*. (1999) and *Koch* (2001).[4]
Sea salt	Not included.	Distributions held fixed in 20th Century at year 2000 values.[2]	Distributions held fixed at 1990 values.	
Dust	Not included.	Distributions held fixed in 20th Century at year 2000 values.[2]	Distributions held fixed at 1990 values.	
Land use change	Distributions held fixed at present-day values.	Distributions held fixed at present-day values.	*Hurtt et al*. (2006) global land use reconstruction history. Includes effect on surface albedo, surface roughness, stomatal resistance, and effective water capacity.	Uses *Ramankutty and Foley* (1999) and *Klein Goldewijk* (2001) time-dependent datasets. Effects on albedo and evapotranspiration included, but no irrigation effects.[4]

Volcanic stratospheric aerosols	*Ammann et al*. (2003).	*Ammann et al*. (2003).	"Blend" between *Sato et al*. (1993) and *Ramachandran et al. (2000).*	Update of *Sato et al*. (1993).
Solar irradiance	*Hoyt and Schatten* (1993).	*Lean et al*. (1995).	*Lean et al*. (1995).	Uses solar spectral changes of *Lean* (2000).

[1]See *Dai et al*. (2001) for further details.
[2]See *Meehl et al*. (2005) for further details.
[3]The chemistry transport model (MOZART; see *Horowitz et al*., 2003; *Tie et al*., 2005) was driven by meteorology from the Middle Atmosphere version of the Community Climate Model ("MACCM"; version 3). "1990" weather from MACCM3 was used for all years between 1860 and 2000.
[4]See *Hansen et al*. (2005a) for further det

One important implication of Table 5.3 is that model-to-model differences in the applied forcings are intertwined with model-to-model differences in the climate *responses* to those forcings. This makes it more difficult to isolate systematic errors that are common to a number of models, or to identify problems with a specific forcing dataset. Note, however, that the lack of a coordinated experimental design is also an advantage, since the "ensemble of opportunity" spans a wide range of uncertainty in current estimates of climate forcings.

In addition to model forcing and response uncertainty, the 20CEN ensemble also encompasses uncertainties arising from inherently unpredictable climate variability. Roughly half of the modeling groups that submitted 20CEN data performed multiple realizations of their historical forcing experiment (see Section 2 and Table 5.1). For example, the five-member ensemble of CCSM3.0 20CEN runs contains an underlying signal (which one might define as the ensemble-average climate response to the forcings varied in CCSM3.0) plus five different sequences of

855 climate noise. Such multi-member ensembles provide valuable information on the relative sizes of
856 signal and noise. In all, a total of 49 20CEN realizations were examined here.
857
858 The following Section presents preliminary results from analyses of these 20CEN runs and the new
859 observational datasets described in Chapters 2-4. Our primary focus is on the tropics, since
860 previous work by *Gaffen et al*. (2000) and *Hegerl and Wallace* (2002) suggests that this is where
861 climate models have significant problems in simulating observed lapse rates changes. We also
862 discuss comparisons of global-mean changes in atmospheric temperatures and lapse rates. We do
863 not discount the importance of comparing models and data at much smaller scales (particularly in
864 view of the incorporation of regional-scale forcing changes in many of the runs analyzed here), but
865 comprehensive regional-scale comparisons were not feasible given the limited time available for
866 completion of this report.
867
868 In order to facilitate "like with like" comparisons between modeled and observed atmospheric
869 temperature changes, we calculate synthetic MSU T_4, T_2, and T_{2LT} from the model 20CEN results
870 (see Chapter, Box 2). Both observed and synthetic MSU T_2 data include a contribution from the
871 cooling stratosphere (*Fu et al*., 2004a,b), and hence complicate the interpretation of slow changes
872 in T_2. To provide a less ambiguous measure of "bulk" tropospheric temperature changes, we use
873 the statistical approach of *Fu et al*. (2004a, 2005) to remove stratospheric influences, thereby
874 obtaining T^*_G and T^*_T in addition to T_{2LT}.[53] As a simple measure of lapse-rate changes, we
875 consider temperature differences between the surface and three different atmospheric layers (T_{2LT},

[53]There is still some debate over the reliability of T^*_G trends estimated with the *Fu et al*. (2004a) statistical approach (*Tett and Thorne*, 2004, *Gillett et al*., 2004; *Kiehl et al*., 2005; *Fu et al*., 2004b; Chapter 4). T^*_T is derived mathematically (from the overlap between the T_4 and T_2 weighting functions) rather than statistically, and is now generally accepted as a reasonable measure of temperature change in the tropical troposphere.

876 T^*_G, and T^*_T). Each of these layers samples slightly different portions of the troposphere (Figure
877 2.2).
878
879 The trend comparisons shown in Sections 5.1 and 5.2 do not involve any formal statistical
880 significance tests (see Statistical Appendix). While such tests are entirely appropriate for
881 comparisons of individual model and observational trends,[54] they are less relevant here, where we
882 compare a 49-member ensemble of model trends with a relatively small number of observationally-
883 based estimates. The model ensemble encapsulates uncertainties in climate forcings and model
884 responses, as well as the effects of climate noise on trends. The observational range characterizes
885 current structural uncertainties in historical changes. We simply assess whether the simulated trend
886 distributions do or do not overlap with these observations. Our goal here is to determine where
887 model results are qualitatively consistent with observations, and where serious inconsistencies are
888 likely to exist. This does not obviate the need for the more rigorous statistical comparisons
889 described in Box 5.5, which should be a high priority (see Recommendations).
890
891 5.1 *Global-Mean Temperature and Lapse-Rate Trends*
892
893 In all but two of the 49 20CEN realizations, the global-mean temperature of the lower stratosphere
894 experiences a net cooling over 1979 to 1999 (Figures 5.2A, 5.3A).[55] The model average T_4 trend is
895 –0.25°C/decade (Table 5.4A). Most of this cooling is due to the combined effects of stratospheric

[54]For example, such tests have been performed by *Santer et al*. (2003b) in comparisons between observed MSU trends (in RSS and UAH) and synthetic MSU trends in four PCM 20CEN realizations.

[55]In the following, all inter-model and model-data comparisons are over January 1979 to December 1999. This is the longest period of overlap (at least during the satellite era) between the model experiments (which generally end in 1999) and the satellite data (which start in 1979).

ozone depletion and increases in well-mixed GHGs (*Ramaswamy et al*., 2001a,b), with the former the dominant influence on T_4 changes over the satellite era (*Ramaswamy et al*., 1996; *Santer et al*., 2003a). The model average cooling is larger (–0.35°C/decade) and closer to the satellite-based estimates if it is calculated from the subset of 20CEN realizations that include forcing by ozone depletion. The range of model T_4 trends encompasses the trends derived from satellites, but not the larger trends estimated from radiosondes. The most likely explanation for this discrepancy is a residual cooling trend in the radiosonde data (Chapter 4).[56] The neglect of stratospheric water vapor increases in most of the 20CEN runs considered here (*Shine et al*., 2003) may be another contributory factor.[57]

[56]Recent work suggests that this residual trend is largest in the lower stratosphere and upper troposphere, and is largely related to temporal changes in the solar heating of the temperature sensors carried by radiosondes (and failure to properly correct for this effect; see *Sherwood et al*., 2005; *Randel and Wu*, 2005).

[57]Recent stratospheric water vapor increases are thought to be partly due to the oxidation of methane, and are expected to have a net cooling effect on T_4. To our knowledge, CH_4-induced stratospheric water vapor increases were explicitly incorporated in only two of the 19 models considered here (GISS-EH and GISS-ER; *Hansen et al.*, 2005a).

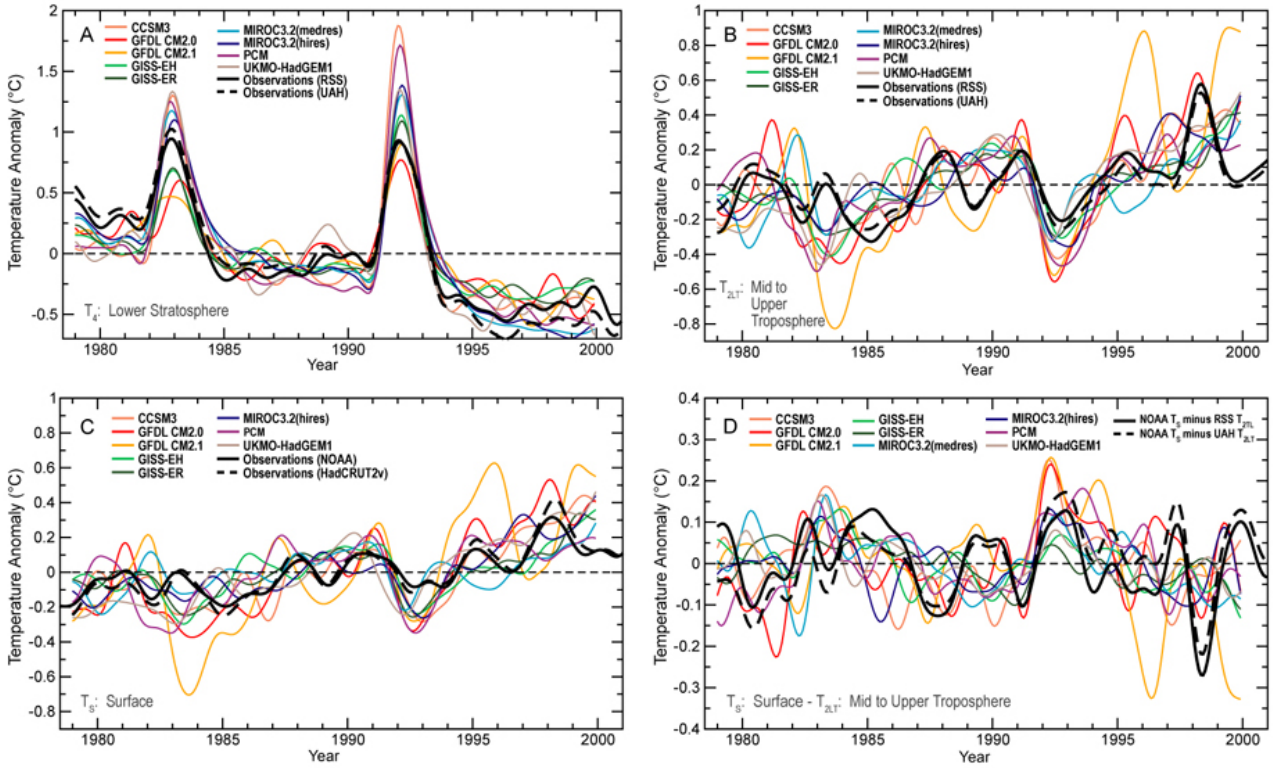

914

915 Figure 5.2A: Modeled and observed changes in global-mean monthly-mean lower stratospheric temperature (T_4). A
916 simple weighting function approach (Box 2.2) was used to calculate a "synthetic" T_4 (equivalent to the MSU T_4
917 monitored by satellites) from model temperature data. Synthetic T_4 results are from "20CEN" experiments performed
918 with nine different models (see Table 5.1). These models were chosen because they satisfy certain minimum
919 requirements in terms of the forcings applied in the 20CEN run: all nine were driven by changes in well-mixed GHGs,
920 sulfate aerosol direct effects, tropospheric and stratospheric ozone, volcanic aerosols, and solar irradiance (in addition
921 to other forcings; see Table 5.2). Observed satellite-based estimates of T_4 changes were obtained from both RSS and
922 UAH (see Chapter 3). All T_4 changes are expressed as departures from a 1979 to 1999 reference period average, and
923 were smoothed with the same filter. To make it easier to compare the variability of T_4 in models with different
924 ensemble sizes (see Table 5.1), only the first 20CEN realization is plotted from each model. This also facilitates
925 comparisons of modeled and observed variability.
926

927 Figure 5.2B: As for Figure 5.2A, but for time series of global-mean, monthly-mean lower tropospheric temperature
928 anomalies (T_{2LT}).
929
930 Figure 5.2C: As for Figure 5.2A, but for time series of global-mean, monthly-mean surface temperature anomalies (T_S).
931
932 Figure 5.2D: As for Figure 5.2A, but for time series of global-mean, monthly-mean temperature differences between
933 the surface and T_{2LT}.
934

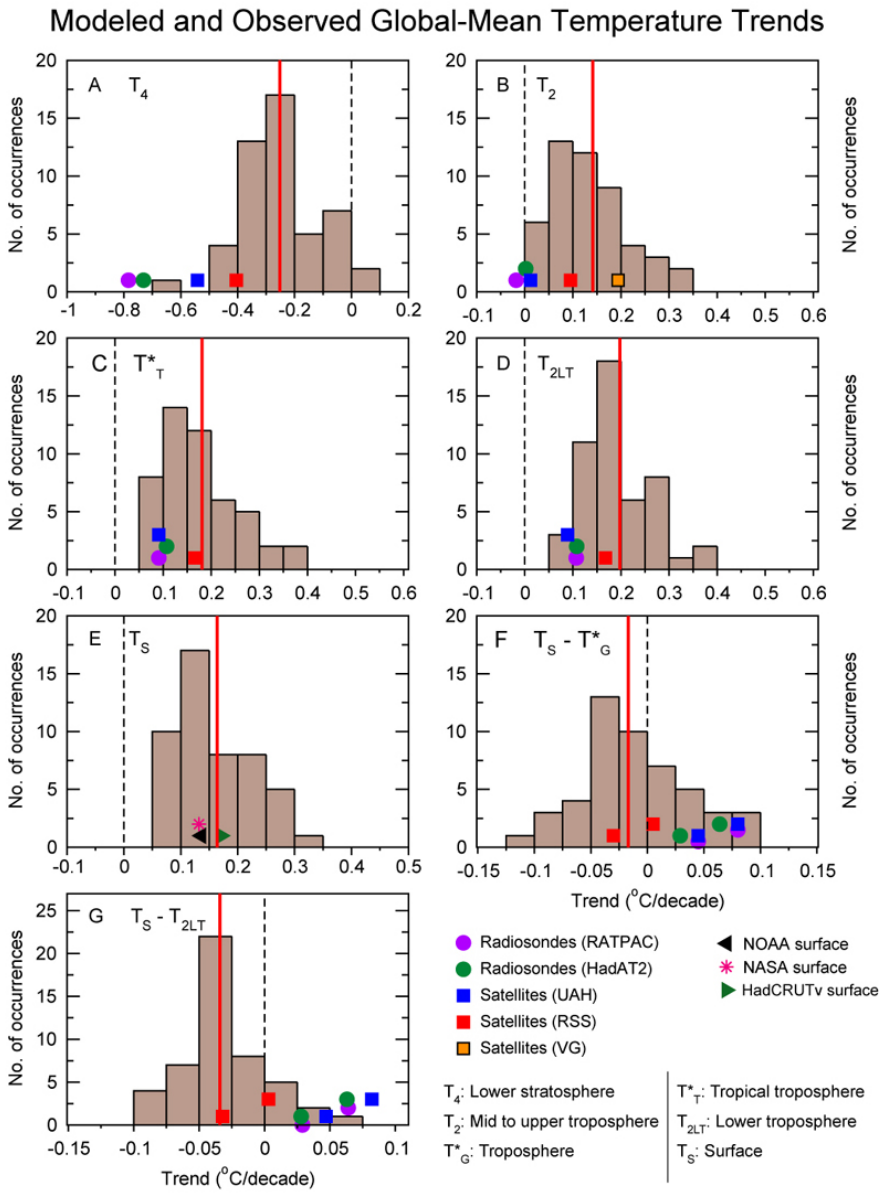

935

936 Figure 5.3: Modeled and observed trends in time series of global-mean T_4 (panel A), T_2 (panel B),
937 T^*_G (panel C), T_{2LT} (panel D), T_S (panel E), T_S minus T^*_G (panel F), and T_S minus T_{2LT}. All trends
938 were calculated using monthly-mean anomaly data. The analysis period is 1979 to 1999. Model
939 results are displayed in the form of histograms. Each histogram is based on results from 49
940 individual realizations of the 20CEN experiment, performed with 19 different models (Table 5.1).
941 The applied forcings are listed in Table 5.2. The vertical red line in each panel is the mean of the
942 model trends, calculated with a sample size of n = 19 (see Table 5.4A). Observed trends are
943 estimated from two radiosonde and three satellite datasets (T_2), two radiosonde and two satellite
944 datasets (T_4, T^*_G and T_{2LT}), and three different surface datasets (T_S) (see Chapter 3). The bottom
945 "rows" of the observed difference trends in panels F and G were calculated with NOAA T_S data.
946 The top "rows" of observed results in F and G were computed with HadCRUT2v T_S data. The
947 vertical offsetting of observed results in these panels (and also in panels B-E) is purely for the

purpose of simplifying the visual display – observed trends bear no relation to the y-axis scale. To simplify the display, the Figure does not show the statistical uncertainties arising from the fitting of linear trends to noisy data. GISS T_S trends (not shown) are very close to those estimated with NOAA T_S data (see Chapter 3).

Table 5.4A: Summary statistics for global-mean temperature trends calculated from 49 different realizations of 20CEN experiments performed with 19 different coupled models. Results are for four different atmospheric layers (T_4, T_2, T^*_G, and T_{2LT}), the surface (T_S), and differences between the surface and the troposphere (T_S minus T^*_G and T_S minus T_{2LT}). All trends were calculated over the 252-month period from January 1979 to December 1999 using global-mean monthly-mean anomaly data. Results are in °C/decade. The values in the "Mean" column correspond to the locations of the red lines in the seven panels of Figure 5.3A. For each layer, means, medians and standard deviations were calculated from a sample size of n = 19, *i.e.*, from ensemble means (if available) and individual realizations (if ensembles were not performed). This avoids placing too much weight on results from a single model with a large number of realizations. Maximum and minimum values were calculated from all available realizations (*i.e.*, from a sample size of n = 49).

Layer	Mean	Median	Std. Dev. (1σ)	Minimum	Maximum
T_4	-0.252	-0.281	0.194	-0.695	0.079
T_2	0.142	0.122	0.079	0.015	0.348
T^*_G	0.181	0.167	0.077	0.052	0.375
T_{2LT}	0.198	0.186	0.070	0.058	0.394
T_S	0.164	0.156	0.062	0.052	0.333
$T_S - T^*_G$	-0.017	-0.017	0.046	-0.110	0.083
$T_S - T_{2LT}$	-0.034	-0.031	0.030	-0.099	0.052

Superimposed on the overall cooling of T_4 are the large stratospheric warming signals in response to the eruptions of El Chichón (in April 1982) and Pinatubo (in June 1991).[58] Nine of the 19 IPCC models explicitly included volcanic aerosols (Figure 5.2A and Table 5.2).[59] Seven of these nine models overestimate the observed stratospheric warming after Pinatubo. GFDL CM2.1 simulates the Pinatubo response reasonably well, but underestimates the response to El Chichón. Differences

[58]These warming signals occur because volcanic aerosols absorb both incoming solar radiation and outgoing thermal radiation (*Ramaswamy et al*., 2001a).

[59]The documentation for the Russian INM-CM3.0 model claims that volcanic aerosols were incorporated in the 20CEN run, but does not show evidence of stratospheric warming signatures after massive volcanic eruptions. This suggests that volcanic cooling effects on surface temperature were implicitly incorporated by changing the surface albedo (a procedure that would not yield volcanically-induced stratospheric warming signals).

970 in the magnitude of the applied volcanic aerosol forcings must account for some of the inter-model
971 differences in the T_4 warming signals (Table 5.3).[60]
972
973 Over 1979 to 1999, the global-mean troposphere warms in all 49 20CEN simulations considered
974 here (Figures 5.2B, 5.3B-D). The shorter-term cooling signals of the El Chichón and Pinatubo
975 eruptions are superimposed on this gradual warming.[61] Because of the influence of stratospheric
976 cooling on T_2, the model average trend is smaller for this layer than for either T_{2LT} or T^*_G, which
977 are more representative of temperature changes in the bulk of the troposphere (Table 5.4A).[62] All of
978 the satellite- and radiosonde-based trends in T_{2LT} and T^*_G are contained within the spread of model
979 results. This illustrates that there is no fundamental discrepancy between modeled and observed
980 trends in global-mean tropospheric temperature.
981
982 In contrast, the T_2 trends in both radiosonde datasets are either slightly negative or close to zero,
983 and are smaller than all of the model results. This difference is most likely due to contamination
984 from residual stratospheric and upper-tropospheric cooling biases in the radiosonde data (Chapter
985 4; *Sherwood et al*., 2005; *Randel and Wu*, 2005). The satellite-based T_2 trends are either close to

[60]More subtle details of the forcing are also relevant to interpretation of inter-model T_4 differences, such as different assumptions regarding the aerosol size distribution, the vertical distribution of the volcanic aerosol relative to the model tropopause, *etc*. Note that observed T_4 changes over the satellite era are not well-described by a simple linear trend, and show evidence of a step-like decline in stratospheric temperatures after the El Chichón and Pinatubo eruptions (*Pawson et al*., 1998; *Seidel and Lanzante*, 2004). Model-model differences in the applied ozone forcings and solar forcings may help to explain why the GFDL, GISS, and HadGEM1 models appear to reproduce some of this step-like behavior, particularly after El Chichón, while T_4 decreases in PCM are much more linear (*Dameris et al*., 2005; *Ramaswamy et al*., 2006).

[61]Because of differences in the timing of modeled and observed ENSO events (Section 5.2), the tropospheric and surface cooling caused by El Chichón is more noticeable in all models than in observations (where it was partially masked by the large 1982/83 El Niño; Figures 5.2B,C).

[62]Because of ozone-induced cooling of the lower stratosphere, the model-average T_2 trend is slightly smaller (0.12°C/decade) and closer to the RSS result if it is estimated from the subset of 20CEN runs that include stratospheric ozone depletion. Subsetting in this way has little impact on the model-average T_{2LT} and T^*_G trends.

the model average (RSS and VG) or just within the model range (UAH; Fig. 5.3B). Even without formal statistical tests, it is clear that observational uncertainty is an important factor in assessing the consistency between modeled and observed changes in mid- to upper tropospheric temperature (*Santer et al.*, 2003b).

Observed T_S trends closely bracket the model average (Figures 5.2C, 5.3E). There is no evidence of a serious inconsistency between modeled and observed surface temperature changes. Structural uncertainties in observed T_S trends are much smaller than for trends in T_4 or tropospheric layer-average temperatures (see Chapter 4).

The model-simulated ranges of lapse-rate trends also encompass virtually all observational results (Figures 5.3F,G).[63] Closer inspection reveals that the model-average trends in tropospheric lapse rate are slightly negative,[64] indicating larger warming aloft than at the surface. Most combinations of observed T_S, T^*_G, and T_{2LT} datasets yield the converse result, and show smaller warming aloft than at the surface. As in the case of global-mean T^*_G and T_{2LT} trends, RSS-based lapse-rate trends are invariably closest to the model average results. Both models and observations show a tendency towards positive values of T_S minus T_{2LT} for several years after the El Chichón and Pinatubo eruptions, indicative of larger cooling aloft than at the surface (Figure 5.2D; Section 5.4).

5.2 *Tropical Temperature and Lapse-Rate Trends*

[63]Note that the subtraction of temperature variability common to surface and troposphere decreases (by about a factor of two) the large range of model trends in T_S, T^*_G, and T_{2LT} (Table 5.4A).

[64]Values are –0.02°C/decade in the case of T_S minus T^*_G and –0.03°C/decade for T_S minus T_{2LT}.

The previous section examined whether simulated global-mean temperature trends were contained within current estimates of structural uncertainty in observations. Since ENSO is primarily a tropical phenomenon, its influence on surface and tropospheric temperature is more pronounced in the tropics than in global averages. Observations contain only one specific sequence of ENSO fluctuations from 1979 to present, and only one sequence of ENSO effects on tropical temperatures. The model 20CEN runs examined here provide many different sequences of ENSO variability. We therefore expect – and find – that these runs yield a wide range of trends in tropical surface and tropospheric temperature (Figure 5.4)[65]. It is of interest whether this large model range encompasses the observed trends.

At the surface, results from the multi-model ensemble include all observational estimates of tropical temperature trends (Figure 5.4E; Table 5.4B). Observed results are close to the model average T_S trend of +0.16°C/decade. There is no evidence that the models significantly over- or underestimate the observed surface warming. In the troposphere, all observational results are still within the range of possible model solutions, but the majority of model results show tropospheric warming that is larger than observed (Figures 5.4B-D). As in the case of the global-mean T_4 trends, the cooling of the tropical stratosphere in both radiosonde datasets is larger than in any of the

[65]This would be true even for a hypothetical "perfect" climate model run with "perfect" forcings. This large model range of tropical temperature trends is not solely due to the effects of ENSO and other modes of internal variability. It also arises from uncertainties in the models and forcings (see Box 5.2 and Table 5.2). Note that the trends discussed here are calculated over a relatively short period of time (several decades).

satellite datasets or model results (Figure 5.4A).[66] The UAH and RSS T_4 trends are close to the model average.[67]

[66]This supports recent findings of a residual cooling bias in tropical radiosonde data (*Sherwood et al*., 2005; *Randel and Wu*, 2005).

[67]The model average is –0.27°C/decade when estimated from the subset of 20CEN runs that include stratospheric ozone depletion.

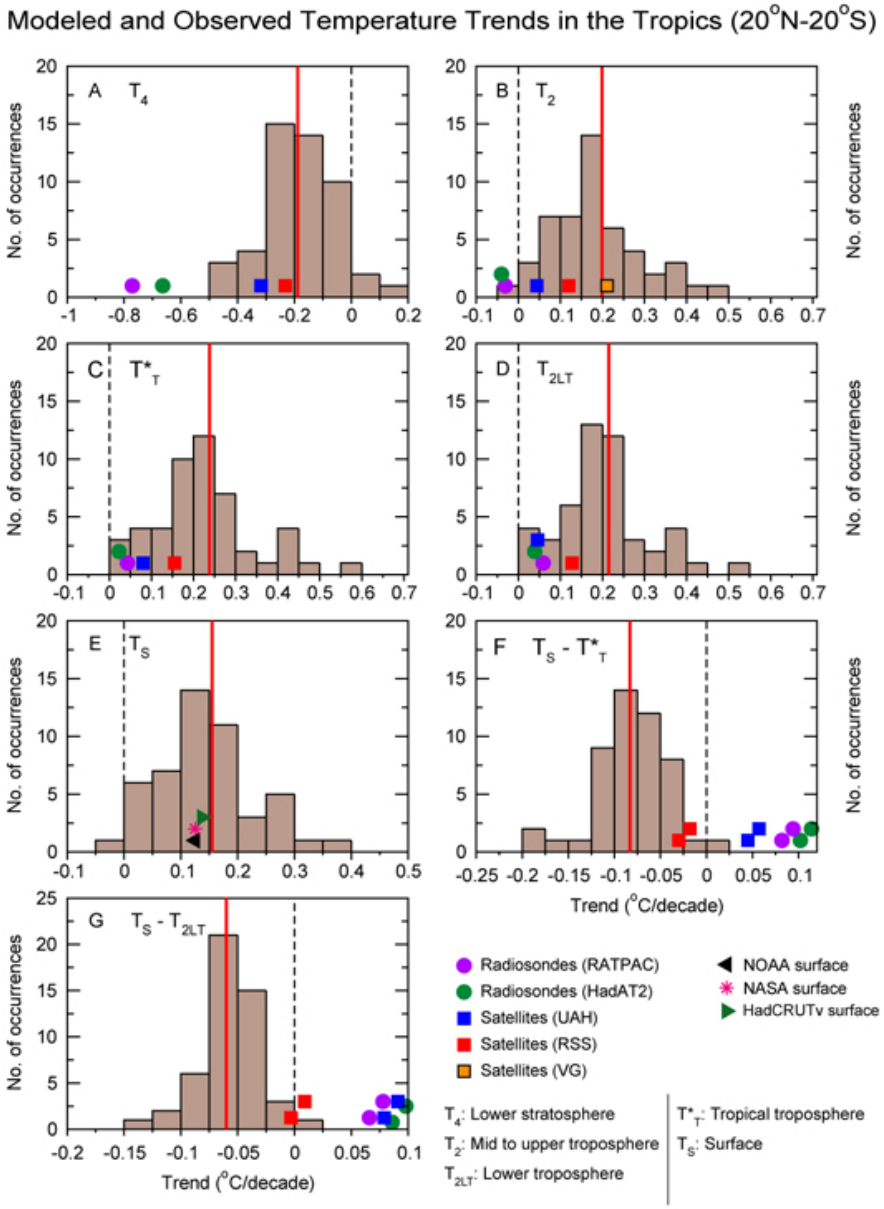

Figure 5.4: As for Figure 5.3, but for trends in the tropics (20°N-20°S).

Table 5.4B: As for Table 5.4A, but for tropical temperature trends (calculated from spatial averages over 20°N-20°S).

Layer	Mean	Median	Std. Dev. (1σ)	Minimum	Maximum
T_4	-0.188	-0.189	0.152	-0.487	0.127
T_2	0.199	0.188	0.098	-0.013	0.481
T^*_T	0.238	0.213	0.105	0.007	0.558
T_{2LT}	0.215	0.194	0.092	0.006	0.509
T_S	0.155	0.144	0.067	-0.017	0.365
$T_S - T^*_T$	-0.083	-0.079	0.040	-0.194	0.017
$T_S - T_{2LT}$	-0.060	-0.053	0.028	-0.145	0.005

In the model results, trends in the two measures of tropical lapse-rate (T_S minus T_{2LT} and T_S minus T^*_T) are almost invariably negative, indicating larger warming aloft than at the surface (Figure 5.4F,G). Similar behavior is evident in only one of the four upper-air datasets examined here (RSS).[68] The RSS trends are just within the range of model solutions.[69] Tropical lapse-rate trends in both radiosonde datasets and in the UAH satellite data are always positive (larger warming at the surface than aloft), and lie outside the range of model results.

This comparison suggests that discrepancies between our current best estimates of simulated and observed lapse-rate changes may be larger and more serious in the tropics than in globally-averaged data. Large structural uncertainties in the observations (even in the sign of the trend in

[68]Note that the VG group do not provide either a stratospheric or lower-tropospheric temperature retrieval, and so could not be included in the comparison of modeled and observed trends in T_S minus T^*_T or T_S minus T_{2LT}.

[69]Three of the four RSS-based results in Figures 5.4F and 5.4G are within two standard deviations of the model average values (see Table 5.4B).

tropical lapse-rate changes) make it difficult to reach more definitive conclusions regarding the significance and importance of model-data discrepancies (see Section 5.4).

5.3 *Spatial Patterns of Lapse-Rate Trends*

Maps of the trends in lower tropospheric lapse rate help to identify geographical regions where the model-data discrepancies in Figures 5.4F and 5.4G are most pronounced. We focus first on four U.S. models: CCSM3.0, PCM, GFDL CM2.1, and GISS-EH (Table 5.3). These show qualitatively similar patterns of trends in T_S minus T_{2LT} (Figures 5.5A-D). Over most of the tropical ocean, the simulated warming is larger in the troposphere than at the surface. All models have some tropical land areas where the surface warms relative to the troposphere. The largest relative warming of the surface occurs at high latitudes in both hemispheres.

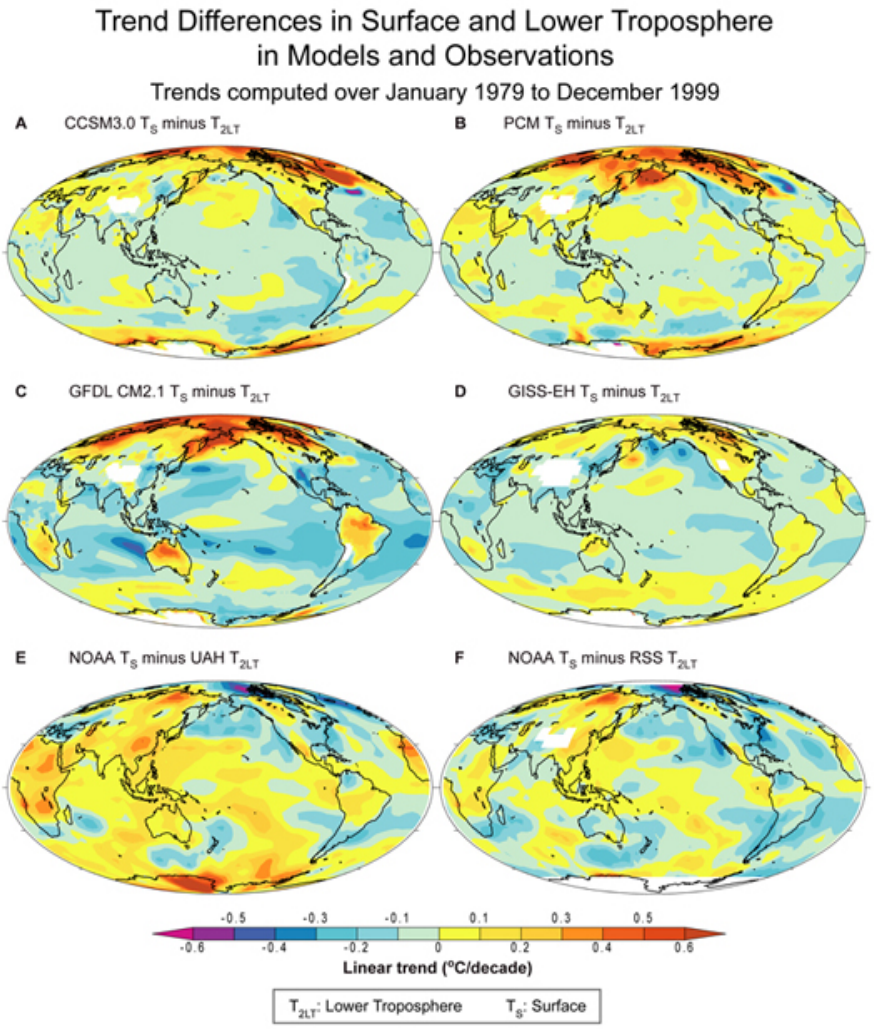

Figure 5.5: Modeled and observed maps of the differences between trends in T_S and T_{2LT}. All trends in T_S and T_{2LT} were calculated over the 252-month period from January 1979 to December 1999. Model results are ensemble means from 20CEN experiments performed with CCSM3.0 (panel A), PCM (panel B), GFDL CM2.1 (panel C), and GISS-EH (panel D). Observed results rely on NOAA T_S trends and on two different satellite estimates of trends in T_{2LT}, obtained from UAH (panel E) and RSS (panel F). White denotes high elevation areas where it is not meaningful to calculate synthetic T_{2LT} (panels A-D). Note that RSS mask T_{2LT} values in such regions, while UAH do not (*c.f.* panels F, E).

To illustrate structural uncertainties in the observed data, we show two different patterns of trends in T_S minus T_{2LT}. Both rely on the same NOAA surface data, but use either UAH (Figure 5.5E) or RSS (Figure 5.5F) as their source of T_{2LT} results. The "NOAA minus UAH" combination provides a picture that is very different from the model results, with coherent warming of the surface relative to the troposphere over much of the world's tropical oceans. While "NOAA minus RSS" also has

relative warming of the surface in the Western and tropical Pacific, it shows relative warming of the *troposphere* in the eastern tropical Pacific and Atlantic Oceans. This helps to clarify why simulated lapse-rate trends in Figures 5.4F and 5.4G are closer to NOAA minus RSS results than to NOAA minus UAH results.

As pointed out by *Santer et al*. (2003b) and *Christy and Spencer* (2003), we cannot use such model-data comparisons alone to determine whether the UAH or RSS T_{2LT} dataset is closer to (an unknown) "reality." As the next section will show, however, models and basic theory can be used to identify aspects of observational behavior that require further investigation, and may help to constrain observational uncertainty.

5.4 *Tropospheric Amplification of Surface Temperature Changes*

When surface and lower tropospheric temperature changes are spatially averaged over the deep tropics, and when day-to-day tropical temperature changes are averaged over months, seasons, or years, it is evident that temperature changes aloft are larger than at the surface. This "amplification" behavior has been described in many observational and modeling studies, and is a consequence of the release of latent heat by moist convecting air (*e.g*., *Manabe and Stouffer*, 1980; *Horel and Wallace*, 1981; *Pan and Oort*, 1983; *Yulaeva and Wallace*, 1994; *Hurrell and Trenberth*, 1998; *Soden*, 2000; *Wentz and Schabel*, 2000; *Hegerl and Wallace*, 2002; *Knutson and Tuleya*, 2004).[70]

[70]The essence of tropical atmospheric dynamics is that the tropics cannot support large temperature gradients, so waves (Kelvin, Rossby, gravity) even out the temperature field between convecting and non-convective regions. The temperature field throughout the tropical troposphere is more or less on the moist adiabat lapse rate set by convection over the warmest waters. This is why there is a trade wind inversion where this profile finds itself inconsistent with boundary layer temperatures in the colder regions.

A recent study by *Santer et al*. (2005) examined this amplification behavior in the same 20CEN runs and observational datasets considered in the present report. The sole difference (relative to the data used here) was that *Santer et al*. analyzed a version of the UAH T_{2LT} data that had not yet been adjusted for a recently-discovered error (*Mears and Wentz*, 2005).[71] The amplification of tropical surface temperature changes was assessed on different timescales (monthly, annual, and multi-decadal) and in different atmospheric layers (T^*_T and T_{2LT}).

On short timescales (month-to-month and year-to-year variations in temperature), the estimated tropospheric amplification of surface temperature changes was in good agreement in all model and observational datasets considered, and was in accord with basic theory. This is illustrated in Figure 5.6, which shows the standard deviations of monthly-mean T_S anomalies plotted against the standard deviations of monthly-mean anomalies of T_{2LT} (panel A) and T^*_T (panel B). All model and observational results lie above the black line indicating equal temperature variability aloft and at the surface. All have similar "amplification factors" between their surface and tropospheric variability.[72] In the models, these similarities occur despite differences in physics, resolution, and forcings, and despite a large range (roughly a factor of 5) in the size of simulated temperature variability. In observations, the scaling ratios estimated from monthly temperature variability are relatively unaffected by the structural uncertainties discussed in Chapter 4.

[71]The error was related to the UAH group's treatment of systematic drifts in the time of day at which satellites sample Earth's diurnal temperature cycle (see Chapter 4).

[72]Note that the slope of the red regression lines that has been fitted to the model results is slightly steeper for T^*_T than for T_{2LT} (*c.f.* panels 5.6A and 5.6B). This is because T^*_T samples more of the mid-troposphere than T_{2LT} (see Prospectus). Amplification is expected to be larger in the mid-troposphere than in the lower troposphere.

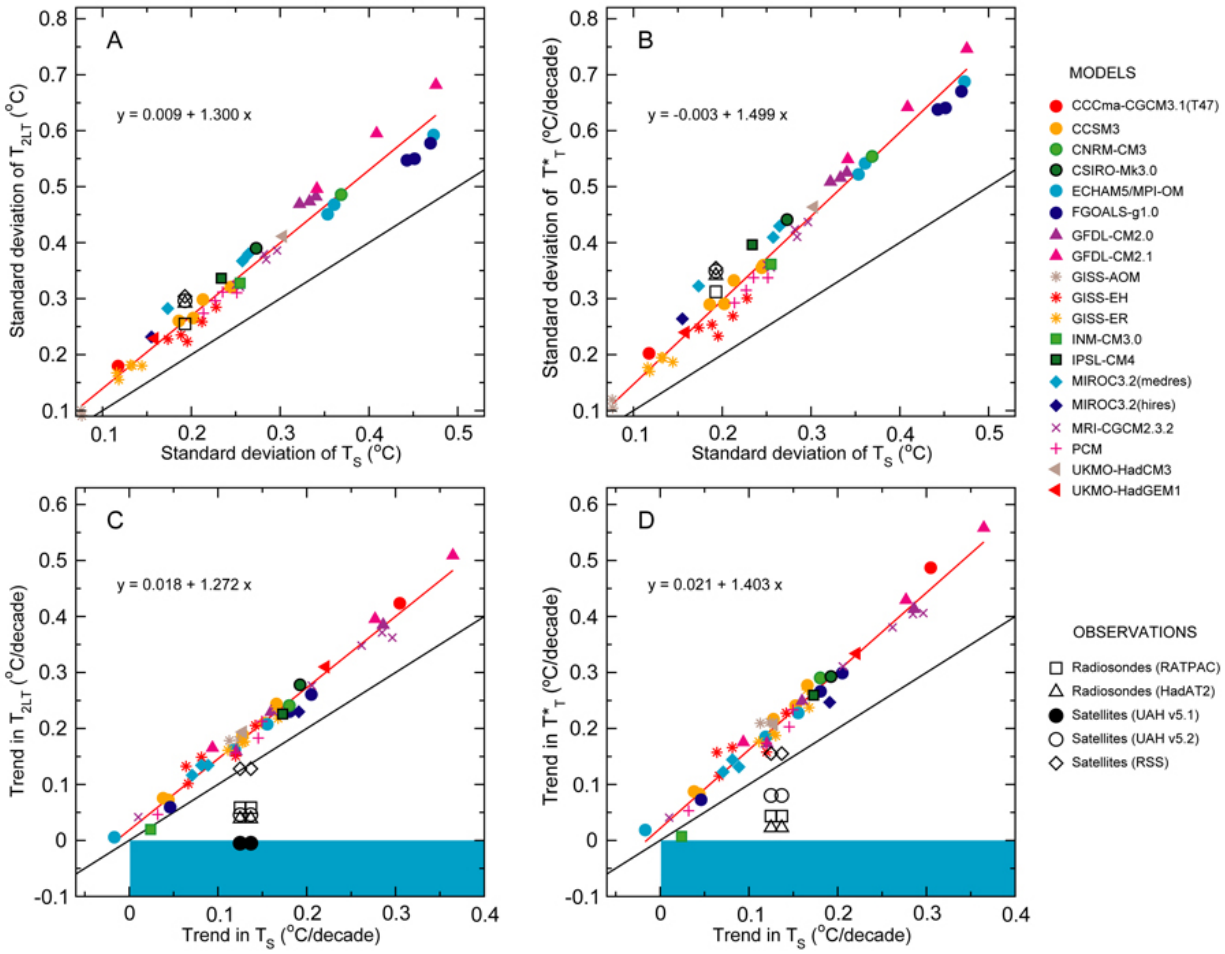

Figure 5.6: Scatter plots showing the relationships between tropical temperature changes at Earth's surface and in two different layers of the troposphere. All results rely on temperature data that have been spatially-averaged over the deep tropics (20°N-20°S). Model data are from 49 realizations of 20CEN runs performed with 19 different models (Table 5.1). Observational results were taken from four different upper-air datasets (two from satellites, and two from radiosondes) and two different surface temperature datasets (see Chapter 3). The two upper panels provide information on the month-to-month variability in T_S and T_{2LT} (panel A) and in T_S and T^*_T (panel B). The two bottom panels consider temperature changes on multi-decadal timescales, and show the trends (over 1979 to 1999) in T_S and T_{2LT} (panel C) and in T_S and T^*_T (panel D). The red line in each panel is the regression line through the model points. Its slope provides information on the amplification of surface temperature variability and trends in the free troposphere. The black line in each panel is given for reference purposes, and has a slope of 1. Values above (below) the black lines indicate tropospheric amplification (damping) of surface temperature changes. There are two columns of observational results in C and D. These are based on the NOAA and HadCRUT2v TS (0.12 and 0.14°C/decade, respectively). Note that panel C show results from published and recently-revised versions of the UAH T_{2LT} data (versions 5.1 and 5.2). Since the standard deviations calculated from NOAA and HadCRUT2v monthly T_S anomalies are very similar, observed results in A and B use NOAA standard deviations only. The blue shading in the bottom two panels defines the region of simultaneous surface warming and tropospheric cooling.

A different picture emerges if amplification behavior is estimated from decadal changes in tropical temperatures. Figures 5.6C and 5.6D show multi-decadal trends in T_S plotted against trends in T_{2LT}

1128 and T^*_T. The 20CEN runs exhibit amplification factors that are consistent with those estimated
1129 from month-to-month and year-to-year temperature variability.[73] Only one observational upper-air
1130 dataset (RSS) shows amplified warming aloft, and similar amplification relationships on short and
1131 on long timescales. The other observational datasets have scaling ratios less than 1, indicating
1132 tropospheric damping of surface warming (*Fu et al*., 2005; *Santer et al*., 2005.[74]
1133
1134 These analyses shed further light on the differences between modeled and observed changes in
1135 tropical lapse rates described in Section 5.2. They illustrate the usefulness of comparing models
1136 and data on different timescales. On short timescales, it is evident that models successfully capture
1137 the basic physics that controls "real world" amplification behavior. On long timescales, model-data
1138 consistency is sensitive to structural uncertainties in the observations. One possible interpretation
1139 of these results is that in the real world, different physical mechanisms govern amplification
1140 processes on short and on long timescales, and models have some common deficiency in
1141 simulating such behavior. If so, these "different physical mechanisms" need to be identified and
1142 understood.
1143
1144 Another interpretation is that the same physical mechanisms control short- and long-term
1145 amplification behavior. Under this interpretation, residual errors in one or more of the observed

[73]As in the case of amplification factors inferred from short-timescale variability, the factors estimated from multi-decadal temperature changes are relatively insensitive to inter-model differences in physics and the applied forcings (see Table 5.3). At first glance, this appears to be a somewhat surprising result in view of the large spatial and temporal heterogeneity of certain forcings (see Section 3). Black carbon aerosols, for example, are thought to cause localized heating of the troposphere relative to the surface (Box 5.3), a potential mechanism for altering amplification behavior. The fact that amplification factors are similar in experiments that include and exclude black carbon aerosols suggests that aerosol-induced tropospheric heating is not destroying the connection of large areas of the tropical ocean to a moist adiabatic lapse rate. Single-forcing experiments (see Recommendations) will be required to improve our understanding of the physical effects of black carbon aerosols and other spatially-heterogeneous forcings on tropical temperature-change profiles.

[74]The previous version of the UAH T_{2LT} data yielded a negative amplification factor for multi-decadal changes in tropical temperatures.

datasets must affect their representation of long-term trends, and must lead to different scaling ratios on short and long timescales. This explanation appears to be the more likely one in view of the large structural uncertainties in observed upper-air datasets (Chapter 4) and the complementary physical evidence supporting recent tropospheric warming (see Section 6).

"Model error" and "observational error" are not mutually exclusive explanations for the amplification results shown in Figures 5.6C and D. Although a definitive resolution of this issue has not yet been achieved, the path towards such resolution is now more obvious. We have learned that models show considerable consistency in terms of what they tell us about tropospheric amplification of surface warming. This consistency holds on a range of different timescales. Observations display consistent amplification behavior on short timescales, but radically different behavior on long timescales. Clearly, not all of the observed lapse-rate trends can be equally probable. Intelligent use of "complementary evidence" – from the behavior of other climate variables, from remote sensing systems other than MSU, and from more systematic exploration of the impacts of different data adjustment choices – should ultimately help us to constrain observational uncertainty, and reach more definitive conclusions regarding the true significance of modeled and observed lapse-rate differences.

5.5 *Vertical Profiles of Atmospheric Temperature Change*

Although formal fingerprint studies have not yet been completed with atmospheric temperature-change patterns estimated from the new 20CEN runs, it is instructive to make a brief qualitative comparison of these patterns. This helps to address the question of whether the inclusion of

previously-neglected forcings (like carbonaceous aerosols and land use/land cover changes; see Section 2) has fundamentally modified the "fingerprint" of human-induced atmospheric temperature changes searched for in previous detection studies.

We examine the zonal-mean profiles of atmospheric temperature change in 20CEN runs performed with four U.S. models (CCSM3, PCM, GFDL CM2.1, and GISS-EH). All four show a common large-scale fingerprint of stratospheric cooling and tropospheric warming over 1979 to 1999 (Figures 5.7A-D). The pattern of temperature change estimated from HadAT2 radiosonde data is broadly similar, although the transition height between stratospheric cooling and tropospheric warming is noticeably lower than in the model simulations (Figure 5.7E). Another noticeable difference is that the HadAT2 data show a relative lack of warming in the tropical troposphere,[75] where all four models simulate maximum warming. This particular aspect of the observed temperature-change pattern is very sensitive to data adjustments (*Sherwood et al*., 2005; *Randel and Wu*, 2005). Tropospheric warming in the observations is most obvious in the NH extratropics, where our confidence in the reliability of radiosonde records is greatest.

[75]Despite the "end point" effect of the large El Niño event in 1997-1998 (see Chapter 3).

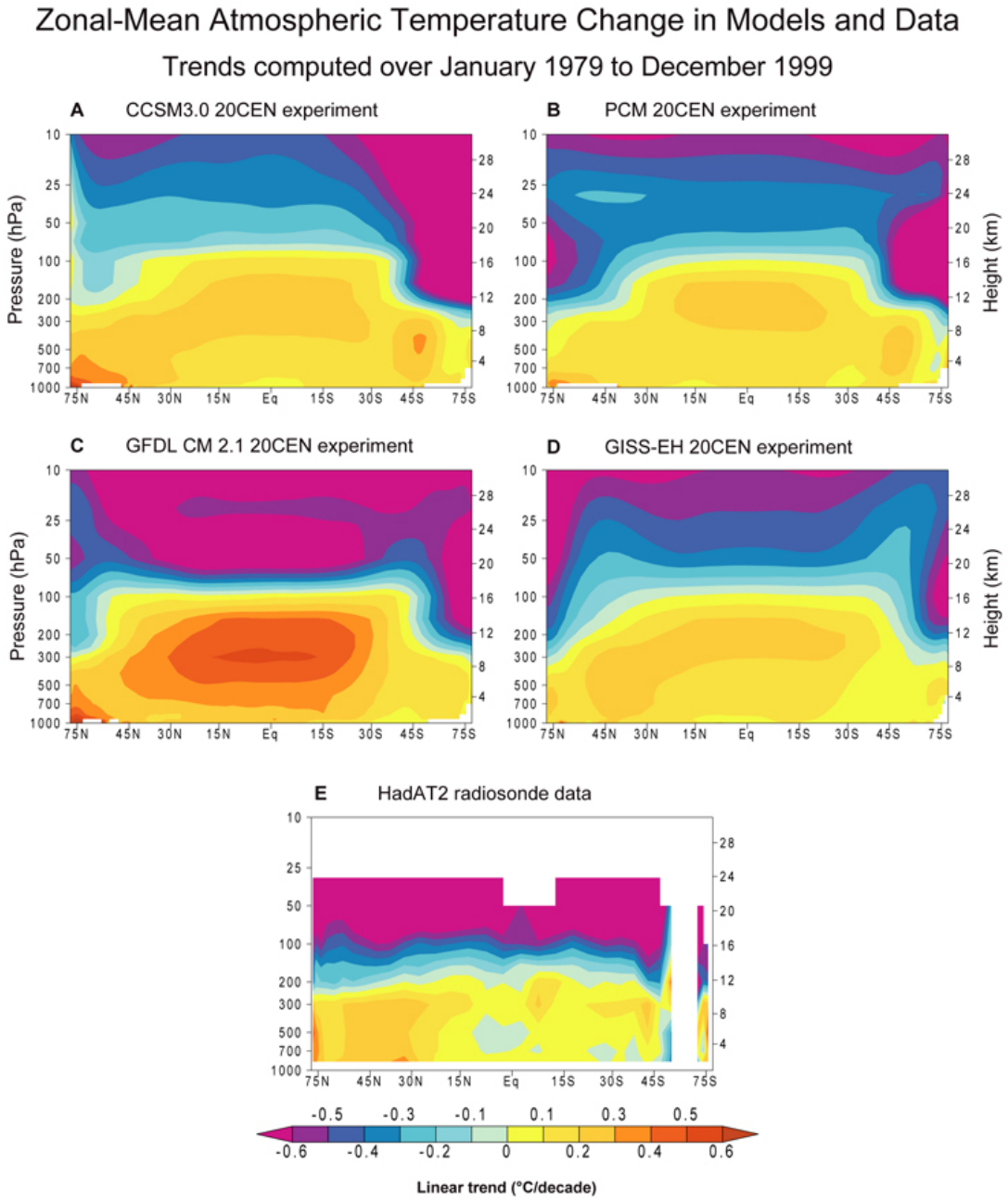

Figure 5.7: Zonal-mean patterns of atmospheric temperature change in "20CEN" experiments performed with four different climate models and in observational radiosonde data. Model results are for CCSM3.0 (panel A), PCM (panel B), GFDL CM 2.1 (panel C), and GISS-EH (panel D). The model experiments are ensemble means. There are differences between the sets of climate forcings that the four models used in their 20CEN runs (Table 5.3). Observed changes (panel E) were estimated with HadAT2 radiosonde data (*Thorne et al.*, 2005, and Chapter 3). The HadAT2 temperature data do not extend above 30 hPa, and have inadequate coverage at high latitudes in the Southern Hemisphere. All temperature changes were calculated from monthly-mean data and are expressed as linear trends (in °C/decade) over 1979 to 1999.

Note that some of the details of the model fingerprint pattern are quite different. For example, GFDL's cooling maximum immediately above the tropical tropopause is not evident in any of the other models. Its maximum warming in the upper tropical troposphere is noticeably larger than in CCSM3.0, PCM, or GISS-EH. While CCSM and GFDL CM2.1 have pronounced hemispheric asymmetry in their stratospheric cooling patterns, with largest cooling at high latitudes in the SH,[76] this asymmetry is less apparent in PCM and GISS-EH.

Future work should consider whether the conclusions of detection studies are robust to such fingerprint differences. This preliminary analysis suggests that the large-scale "fingerprint" of stratospheric cooling and tropospheric warming over the satellite era – a robust feature of previous detection work – has not been fundamentally altered by the inclusion of hitherto-neglected forcings like carbonaceous aerosols and LULC changes (see Table 5.3). This does not diminish the need to quantify the individual contributions of these forcings in appropriate "single forcing" experiments.

6 *Changes in "Complementary" Climate Variables*

Body temperature is a simple metric of our physical well-being. A temperature of 40°C (104°F) is indicative of an illness, but does not by itself identify the cause of the illness. In medicine, investigation of causality typically requires the analysis of many different lines of evidence. Similarly, analyses of temperature alone provide incomplete information on the causes of climate change. For example, there is evidence that major volcanic eruptions affect not only the Earth's

[76]This may be related to an asymmetry in the pattern of stratospheric ozone depletion: the largest ozone decreases over the past 2-3 decades have occurred at high latitudes in the SH.

radiation budget (*Wielicki et al*., 2002; *Soden et al*., 2002) and atmospheric temperatures (*Hansen et al*., 1997, 2002; *Free and Angell*, 2002; *Wigley et al*., 2005a), but also water vapor (*Soden et al*., 2002), precipitation (*Gillett et al*., 2004c), atmospheric circulation patterns (see, *e.g*., *Robock*, 2000, and *Ramaswamy et al*., 2001a; *Robock and Oppenheimer*, 2003), ocean heat content and sea level (*Church et al*., 2005), and even global-mean surface pressure (*Trenberth and Smith*, 2005). These responses are physically interpretable and internally consistent.[77] The combined evidence from changes in all of these variables makes a stronger case for an identifiable volcanic effect on climate than evidence from a single variable only.

A "multi-variable" perspective may also be beneficial in understanding the possible causes of differential warming. The value of "complementary" climate datasets for studying this specific problem has been recognized by *Pielke* (2004) and by *Wentz and Schabel* (2000). The latter found internally-consistent increases in SST, T_{2LT}, and marine total column water vapor over the 12-year period from 1987 to 1998.[78] Multi-decadal increases in surface and lower tropospheric water vapor were also reported in the IPCC Second Assessment Report (*Folland et al*., 2001).[79] More recently,

[77]The physical consistency between the temperature and water vapor changes after the Pinatubo eruption has been clearly demonstrated by *Soden et al*. (2002). The surface and tropospheric cooling induced by Pinatubo caused a global-scale reduction in total column water vapor. Since water vapor is a strong GHG, the reduction in water vapor led to less trapping of outgoing thermal radiation by Earth's atmosphere, thus *amplifying* the volcanic cooling. This is referred to as a "positive feedback." *Soden et al*. "disabled" this feedback in a climate model experiment, and found that the "no water vapor feedback" model was incapable of simulating the observed tropospheric cooling after Pinatubo. Inclusion of the water vapor feedback yielded close agreement between the simulated and observed T_{2LT} responses to Pinatubo. This suggests that the model used by *Soden et al*. captures important aspects of the physics linking the real world's temperature and moisture changes.

[78]The Wentz and Schabel study used NOAA optimally-interpolated SST data, a version of the UAH T_{2LT} data that had been corrected for orbital decay effects, and information on total column water vapor from the satellite-based Special Sensor Microwave Imager (SSM/I).

[79]More specifically, *Folland et al*. (2001) concluded that "Changes in water vapour mixing ratio have been analysed for selected regions using *in situ* surface observations as well as lower-tropospheric measurements based on satellites and weather balloons. A pattern of overall surface and lower-tropospheric water vapour mixing ratio increases over the past few decades is emerging, although there are likely to be some time-dependent biases in these data and regional variations in trends. The more reliable data sets show that it is likely that total atmospheric water vapour has increased

Trenberth et al. (2005) found significant increases in total column water vapor over the global ocean.[80] At constant relative humidity, water vapor increases nonlinearly with increasing temperature (*Hess*, 1959). Slow increases in tropospheric water vapor therefore provide circumstantial evidence in support of tropospheric warming. However, water vapor measurements are affected by many of the same data quality and temporal homogeneity problems that influence temperature measurements (*Elliott*, 1995; *Trenberth et al*., 2005), so the strength of this circumstantial evidence is still questionable.[81]

Other climate variables also corroborate the warming of Earth's surface over the second half of the 20th Century. Examples include increases in ocean heat content (*Levitus et al*., 2000, 2005; *Willis* et al., 2004), sea-level rise (*Cabanes et al*., 2001), thinning of major ice sheets and ice shelves (*Krabill et al*., 1999; *Rignot and Thomas*, 2002; *Domack et al*., 2005), and widespread glacial retreat, with accelerated rates of glacial retreat over the last several decades (*Arendt et al*., 2002; *Paul et al.,* 2004).[82]

several per cent per decade over many regions of the Northern Hemisphere since the early 1970s. Changes over the Southern Hemisphere cannot yet be assessed".

[80]*Trenberth et al*. (2005) reported an increase in total column water vapor over 1988 to 2001 of "1.3 ± 0.3% per decade for the ocean as a whole, where the error bars are 95% confidence intervals." This estimate was obtained with an updated version of the SSM/I dataset analyzed by *Wentz and Schabel* (2000).

[81]Note, however, that SSM/I-derived water vapor measurements may have some advantages relative to temperature measurements obtained from MSU. *Wentz and Schabel* (2000) point out that (under a constant relative humidity assumption), the 22 GHz water vapor radiance observed by SSM/I is three times more sensitive to changes in air temperature than the MSU T_2 54 GHz radiance. Furthermore, while drift in sampling the diurnal cycle influences MSU-derived tropospheric temperatures (Chapter 4), it has a much smaller impact on SSM/I water vapor measurements.

[82]*Folland et al*. (2001) note that "Long-term monitoring of glacier extent provides abundant evidence that tropical glaciers are receding at an increasing rate in all tropical mountain areas". Accelerated retreat of high-elevation tropical glaciers is occurring within the tropical lower tropospheric layer that is a primary focus of this report, and provides circumstantial support for warming of this layer over the satellite era".

Changes in some of these "complementary" variables have been used in detection and attribution studies. Much of this work has focused on ocean heat content. When driven by anthropogenic forcing, a number of different CGCMs capture the overall increase in observed ocean heat content estimated by *Levitus et al*. (2000; 2005), but not the large decadal variability in heat content (*Barnett et al*., 2001; *Levitus et al*., 2001; *Reichert et al*., 2002; *Sun and Hansen*, 2003; *Pielke*, 2003; *Gregory et al*., 2004; *Hansen et al*., 2005b).[83] It is still unclear whether this discrepancy between simulated and observed variability is primarily due to model deficiencies or is an artifact of how *Levitus et al*. (2000; 2005) "infilled" data-sparse ocean regions (*Gregory et al*., 2004; *AchutaRao et al*., 2005).

In summary, the behavior of complementary variables enhances our confidence in the reality of large-scale warming of the Earth's surface, and tells us that the signature of this warming is manifest in many different aspects of the climate system. Pattern-based fingerprint detection work performed with ocean heat content (*Barnett et al*., 2001; *Reichert et al*., 2002; *Barnett et al*., 2005; *Pierce et al*., 2005), sea-level pressure (*Gillett et al.,* 2003), and tropopause height (*Santer et al*., 2003a, 2004) suggests that anthropogenic forcing is necessary in order to explain observed changes in these variables. This supports the findings of the surface- and atmospheric temperature studies described in Section 4.4. To date, however, investigations of complementary variables have not enabled us to narrow uncertainties in satellite- and radiosonde-based estimates of tropospheric temperature change over the past two-and-a-half decades.[84] Formal detection and attribution studies

[83]Model control runs cannot generate such large multi-decadal increases in the heat content of the global ocean.

[84]The tropopause is the transition zone between the turbulently-mixed troposphere, where most weather occurs, and the more stably-stratified stratosphere (see Preface and Chapter 1). Increases in tropopause height over the past 3-4 decades represent an integrated response to temperature changes above and below the tropopause (*Highwood et al*., 2000; *Santer et al*., 2004), and are evident in both radiosonde data (*Highwood et al*., 2000; *Seidel et al*., 2001) and reanalyses (*Randel et al*., 2000). In model 20CEN simulations, recent increases in tropopause height are driven by the

involving water vapor changes may be helpful in this regard, since observations suggest a recent moistening of the troposphere, consistent with tropospheric warming.

7 *Summary*

This chapter has evaluated a wide range of scientific literature dealing with the possible causes of recent temperature changes, both at the Earth's surface and in the free atmosphere. It shows that many factors – both natural and human-related – have probably contributed to these changes. Quantifying the relative importance of these different climate forcings is a difficult task. Analyses of observations alone cannot provide us with definitive answers. This is because there are important uncertainties in the observations and in the climate forcings that have affected them. Although computer models of the climate system are useful in studying cause-effect relationships, they, too, have limitations. Advancing our understanding of the causes of recent lapse-rate changes will best be achieved by comprehensive comparisons of observations, models, and theory – it is unlikely to arise from analysis of a single model or observational dataset.

combined effects of GHG-induced tropospheric warming and ozone-induced stratospheric cooling (*Santer et al*., 2003a). Available reanalysis products do not provide a consistent picture of the relative contributions of stratospheric and tropospheric temperature changes to recent tropopause height increases (*Pielke and Chase*, 2004; *Santer et al*., 2004).

References

AchutaRao, K.M., *et al*., 2005: Variability of ocean heat uptake: Reconciling observations and models. *Journal of Geophysical Research (Oceans)* (in press).

Allen, M.R., *et al*., 2005: Quantifying anthropogenic influence on recent near-surface temperature. *Surveys in Geophysics* (in press).

Allen, M.R., and D.A. Stainforth, 2002: Towards objective probabilistic climate forecasting. *Nature*, **419**, 228.

Allen, M., 1999: Do-it-yourself climate prediction. *Nature*, **401**, 642.

Allen, M.R., and S.F.B. Tett, 1999: Checking for model consistency in optimal fingerprinting. *Climate Dynamics*, **15**, 419-434.

Ammann, C.M., *et al*., 2003: A monthly and latitudinally varying forcing dataset in simulations of 20th century climate. *Geophysical Research Letters*, **30**, 1657, doi:10.1029/2003GL016875.

Andronova, N.G., and M.E. Schlesinger, 2001: Objective estimation of the probability density function for climate sensitivity. *Journal of Geophysical Research (Atmospheres)*, **106**, 22605-22611.

Andronova, N.G., *et al*., 1999: Radiative forcing by volcanic aerosols from 1850 to 1994. *Journal of Geophysical Research (Atmospheres)*, **104**, 16807-16826.

Arendt, A.A., *et al*., 2002: Rapid wastage of Alaska glaciers and their contribution to rising sea level. *Science*, **297**, 382-386.

Barnett, T.P. *et al*., 2005: Penetration of human-induced warming into the world's oceans. *Science*, **309**, 284-287.

Barnett, T.P., D.W. Pierce, and R. Schnur, 2001: Detection of anthropogenic climate change in the world's oceans. *Science*, **292**, 270-274.

Barnett, T.P., and M.E. Schlesinger, 1987: Detecting changes in global climate induced by greenhouse gases. *Journal of Geophysical Research (Atmospheres)*, 92, 14772-14780.

Bengtsson, L., E. Roeckner, and M. Stendel, 1999: Why is the global warming proceeding much slower than expected? *Journal of Geophysical Research (Atmospheres)*, **104**, 3865-3876.

Brown, S.J., *et al*., 2000: Decadal variability in the lower-tropospheric lapse rate. *Geophysical Research Letters*, **27**, 997-1000.

Brovkin, V., *et al*., 2004: Role of land cover changes for atmospheric CO_2 increase and climate change during the last 150 years. *Global Change Biology*, **10**, 1253-1266.

Cabanes, C., A. Cazenave, and C. Le Provost, 2001: Sea level rise during past 40 years determined from satellite and in situ observations. *Science*, **294**, 840-842.

Chase, T.N., *et al*., 2004: Likelihood of rapidly increasing surface temperatures unaccompanied by strong warming in the free troposphere. *Climate Research*, **25**, 185-190.

Christy, J.R., and R.T. McNider, 1994: Satellite greenhouse signal. *Nature*, **367**, 325.

Christy, J.R., and R. Spencer, 2003: Reliability of satellite data sets. *Science*, **301**, 1046-1047.

Christy, J.R., *et al*., 2003: Error estimates of version 5.0 of MSU-AMSU bulk atmospheric temperatures. *Journal of Atmospheric and Oceanic Technology*, **20**, 613-629.

Church, J.A., N.J. White, and J.M. Arblaster, 2005: Significant decadal-scale impact of volcanic eruptions on sea level and ocean heat content. *Nature*, **438**, doi:10.1038/nature04237.

Collins, W.D., *et al*., 2005: The Community Climate System Model: CCSM3. *Journal of Climate (accepted).*

Crowley, T.J., 2000: Causes of climate change over the past 1,000 years. *Science*, **289**, 270-277.

Dai., A., *et al.,* 2001: Climates of the Twentieth and Twenty-First centuries simulated by the NCAR Climate System Model. *Journal of Climate*, **14**, 485-519.

Dameris, M., *et al*., 2005: Long-term changes and variability in a transient simulation with a chemistry-climate model employing realistic forcing. *Atmospheric Chemistry and Physics*, **5**, 2121-2145.

Delworth, T.L., *et al*., 2005: GFDL's CM2 global coupled climate models – Part 1: Formulation and simulation characteristics. *Journal of Climate* (in press).

Domack, E., *et al*., 2005: Stability of the Larsen B ice shelf on the Antarctic Peninsula during the Holocene epoch. *Nature*, **436**, 681-685.

Douglass, D.H., and R.S. Knox, 2005: Climate forcing by the volcanic eruption of Mount Pinatubo. *Geophysical Research Letters*, **32**, L05710, doi:10.1029/2004GL022119.

Douglass, D.H., B.D. Pearson, and S.F. Singer, 2004: Altitude dependence of atmospheric temperature trends: Climate models versus observation. *Geophysical Research Letters*, **31**, doi:10.1029/2004GL020103.

Douglass, D.H., and B.D. Clader, 2002: Climate sensitivity of the Earth to solar irradiance. *Geophysical Research Letters*, **29**, doi:10.1029/2002GL015345.

1374 Elliott, W.P., 1995: On detecting long-term changes in atmospheric moisture. *Climatic Change*, **31**,
1375 349-367.
1376
1377 Feddema, J., *et al*., 2005: An evaluation of GCM sensitivity to land cover change experiments, and
1378 their potential importance to IPCC scenario simulations. *Journal of Climate* (accepted).
1379
1380 Free, M., and J.K. Angell, 2002: Effect of volcanoes on the vertical temperature profile in
1381 radiosonde data. *Journal of Geophysical Research (Atmospheres)*, **107**,
1382 doi:10.1029/2001JD001128.
1383
1384 Folland, C.K., *et al*., 2001: Observed climate variability and change. In: *Climate Change 2001: The*
1385 *Scientific Basis. Contribution of Working Group I to the Third Assessment Report of the*
1386 *Intergovernmental Panel on Climate Change* [Houghton, J.T., *et al*., (eds.)]. Cambridge
1387 University Press, Cambridge, United Kingdom and New York, NY, USA, 881 pp.
1388
1389 Folland, C.K., *et al*., 1998: Influences of anthropogenic and oceanic forcing on recent climate
1390 change. *Geophysical Research Letters*, **25**, 353-356.
1391
1392 Forest, C.E., *et al*., 2002: Quantifying uncertainties in climate system properties with the use of
1393 recent climate observations. *Science*, **295**, 113-117.
1394
1395 Forest, C.E., *et al*., 2001: Constraining climate model properties using optimal fingerprint detection
1396 studies. *Climate Dynamics*, **18**, 277-295.
1397
1398 Fu, Q., and C.M. Johanson, 2005: Satellite-derived vertical dependence of tropical tropospheric
1399 temperature trends. *Geophysical Research Letters*, **32**, L10703,
1400 doi:10.1029/2004GL022266.
1401
1402 Fu, Q., *et al*., 2004a: Contribution of stratospheric cooling to satellite-inferred tropospheric
1403 temperature trends. *Nature*, **429**, 55-58.
1404
1405 Fu, Q., *et al*., 2004b: Reply to "Tropospheric temperature series from satellites" and "Stratospheric
1406 cooling and the troposphere". *Nature*, doi:10.1038/nature03208.
1407
1408 Gaffen, D.J., *et al*., 2000: Multidecadal changes in the vertical structure of the tropical troposphere.
1409 *Science*, **287**, 1242-1245.
1410
1411 Gates, W.L., *et al*., 1999: An overview of the results of the Atmospheric Model Intercomparison
1412 Project (AMIP I). *Bulletin of the American Meteorological Society*, **80**, 29-55.
1413
1414 Gillett, N.P. *et al*., 2004a: Testing the linearity of the response to combined greenhouse gas and
1415 sulfate aerosol forcing. *Geophysical Research Letters*, **31**, L14201,
1416 doi:10.1029/2004GL020111.
1417

Gillett, N.P., B.D. Santer, and A.J. Weaver, 2004b: Quantifying the influence of stratospheric cooling on satellite-derived tropospheric temperature trends. *Nature*, doi:10.1038/nature03209.

Gillett, N.P., *et al*., 2004c: Detection of volcanic influence on global precipitation. *Geophysical Research Letters*, **31**, doi:10.1029/2004GL020044.

Gillett, N.P., *et al*., 2003: Detection of human influence on sea level pressure. *Nature*, **422**, 292-294.

Gillett, N.P., M.R. Allen, and S.F.B. Tett, 2000: Modelled and observed variability in atmospheric vertical temperature structure. *Climate Dynamics*, **16**, 49-61.

Gregory, J.M., *et al*., 2004: Simulated and observed decadal variability in ocean heat content. *Geophysical Research Letters*, **31**, L15312, doi:10.1029/2004GL020258.

Gregory, J.M., *et al*., 2002: An observationally based estimate of the climate sensitivity. *Journal of Climate*, **15**, 3117-3121.

Grody, N.C., *et al*., 2004: Calibration of multisatellite observations for climatic studies: Microwave Sounding Unit (MSU). *Journal of Geophysical Research (Atmospheres)*, **109**, D24104, doi:10.1029/2004JD005079.

Haigh, J.D., 1994: The role of stratospheric ozone in modulating the solar radiative forcing of climate. *Nature*, **370**, 544-546.

Hansen, J., *et al*., 2005a: Efficacy of climate forcings. *Journal of Geophysical Research (Atmospheres)*, **110**, D18104, doi:10.1029/2005JD005776.

Hansen, J., *et al*., 2005b: Earth's energy imbalance: Confirmation and implications. *Science*, **308**, 1431-1435.

Hansen, J., and L. Nazarenko, 2003: Soot climate forcing via snow and ice albedos. *Proceedings of the National Academy of Sciences*, **101**, 423-428, doi:10.1073/pnas.2237157100.

Hansen, J., 2002: A brighter future. *Climatic Change*, **52**, 435-440.

Hansen, J., *et al*., 2002: Climate forcings in Goddard Institute for Space Studies SI2000 simulations. *Journal of Geophysical Research (Atmospheres)*, **107**, doi:10.1029/20001JD001143.

Hansen, J., *et al*., 2000: Global warming in the Twenty-First Century: An alternative scenario. *Proceedings of the National Academy of Sciences*, **97**, 9875-9880.

Hansen, J., *et al*., 1997: Forcings and chaos in interannual to decadal climate change. *Journal of Geophysical Research (Atmospheres)*, **102**, 25679-25720.

Hansen, J., *et al*., 1995: Satellite and surface temperature data at odds? *Climatic Change*, **30**, 103-117.

Hansen, J., *et al*., 1993: How sensitive is the Earth's Climate? *Natl. Geog. Res. Explor*., **9**, 142-158.

Harvey, L.D.D., and R.K. Kaufmann, 2002: Simultaneously constraining climate sensitivity and aerosol radiative forcing. *Journal of Climate*, **15**, 2837-2861.

Hasselmann, K., 1997: Multi-pattern fingerprint method for detection and attribution of climate change. *Climate Dynamics*, **13**, 601-612.

Hasselmann, K., 1993: Optimal fingerprints for the detection of time dependent climate change. *Journal of Climate*, **6**, 1957-1971.

Hasselmann, K., 1979: In: *Meteorology of Tropical Oceans* (Ed. D.B. Shaw). Royal Meteorological Society of London, London, U.K., pp. 251-259.

Hegerl, G.C., and J.M. Wallace, 2002: Influence of patterns of climate variability on the difference between satellite and surface temperature trends. *Journal of Climate*, **15**, 2412-2428.

Hegerl, G.C., *et al*., 1997: Multi-fingerprint detection and attribution of greenhouse-gas- and aerosol-forced climate change. *Climate Dynamics*, **16**, 737-754.

Hegerl, G.C., *et al*., 1996: Detecting greenhouse-gas-induced climate change with an optimal fingerprint method. *Journal of Climate*, **9**, 2281-2306.

Hess, S.L., 1959: *Introduction to Theoretical Meteorology*. Holt, Rinehart and Winston, New York, 362 pp.

Highwood, E.J., B.J. Hoskins, and P. Berrisford, 2000: Properties of the Arctic tropopause. *Quarterly Journal of the Royal Meteorological Society*, **126**, 1515-1532.

Hoffert, M.I., and C. Covey, 1992: Deriving global climate sensitivity from paleoclimate reconstructions. *Nature*, **360**, 573-576.

Horel, J.D., and J.M. Wallace, 1981: Planetary-scale atmospheric phenomena associated with the Southern Oscillation. *Monthly Weather Review*, **109**, 813-829.

Horowitz, L.W. *et al*., 2003: A global simulation of tropospheric ozone and related tracers: Description and evaluation of MOZART, version 2, *Journal of Geophysical Research (Atmospheres)*, **108**, 4784, doi:10.1029/2002JD002853.

Houghton, J.T., *et al*., 2001: *Climate Change 2001: The Scientific Basis*. Cambridge University Press, Cambridge, U.K., 881 pp.

Hoyt, D.V., and K.H. Schatten, 1993: A discussion of plausible solar irradiance variations, 1700-1992. *Journal of Geophysical Research (Atmospheres)*, **98**, 18895-18906.

Hurrell, J.W., *et al*., 2003: *The North Atlantic Oscillation: Climatic Significance and Environmental Impact*. American Geophysical Union, Geophysical Monograph 134, 279 pp.

Hurrell, J.W., and K.E. Trenberth, 1998: Difficulties in obtaining reliable temperature records: Reconciling the surface and satellite Microwave Sounding Unit records. *Journal of Climate*, **11**, 945-967.

Hurtt, G., *et al*., 2006: Three centuries of gridded, global land-use transition rates and wood harvest statistics for Earth System Model applications. *Global Change Biology* (submitted).

International Detection and Attribution Group (IDAG), 2005: Detecting and attributing external influences on the climate system: A review of recent advances. *Journal of Climate*, **18**, 1291-1314.

Jacobson, M.Z., 2004: Climate response of fossil fuel and biofuel soot, accounting for soot's feedback to snow and sea ice albedo and emissivity. *Journal of Geophysical Research (Atmospheres)*, **109**, D21201, doi:10.1029/2004JD004945.

Jones, P.D., *et al*., 2003: Surface climate responses to explosive volcanic eruptions seen in long European temperature records and mid-to-high latitude tree-ring density around the Northern Hemisphere. In: *Volcanism and the Earth's Atmosphere*, A. Robock and C. Oppenheimer (Eds.), AGU Geophysical Monograph Series, **139**, Washington D.C. American Geophysical Union, 239-254.

Jones, P.D., *et al*., 2001: Adjusting for sampling density in grid box land and ocean surface temperature time series. *Journal of Geophysical Research (Atmospheres)*, **106**, 3371-3380.

Jones, P.D., *et al*., 1999: Surface air temperature and its changes over the past 150 years. *Reviews of Geophysics*, **37**, 173-199.

Jones, P.D., 1994: Recent warming in global temperature series. *Geophysical Research Letters*, **21**, 1149-1152.

Jones, G.S., S.F.B. Tett, and P.A. Stott, 2003: Causes of atmospheric temperature change 1960-2000: A combined attribution analysis. *Geophysical Research Letters*, **30**, doi:10.1029/2002GL016377.

Karoly, D.J., and Q. Wu, 2005: Detection of regional surface temperature trends. *Journal of Climate* (submitted).

Karoly, D.J., *et al*., 2003: Detection of a human influence on North American climate. *Science*, **302**, 1200-1203.

Karoly, D.J., *et al*., 1994: An example of fingerprint detection of greenhouse climate change. *Climate Dynamics*, **10**, 97-105.

Kiehl, J.T., J.M. Caron, and J.J. Hack, 2005: On using global climate model simulations to assess the accuracy of MSU retrieval methods for tropospheric warming trends. *Journal of Climate*, **18**, 2533-2539.

Klein Goldewijk, K., 2001: Estimating global land use change over the past 300 years: The HYDE database. *Global Biogeochemical Cycles*, **15**, 417-433.

Knutson, T.R., and R.E. Tuleya, 2004: Impact of CO_2-induced warming on simulated hurricane intensity and precipitation: Sensitivity to the choice of climate model and convective parameterization. *Journal of Climate*, **17**, 3477-3495.

Koch, D., 2001: Transport and direct radiative forcing of carbonaceous and sulfate aerosols in the GISS GCM. *Journal of Geophysical Research (Atmospheres)*, **106**, 20311-20332.

Koch, D., *et al*., 1999: Tropospheric sulfur simulation and sulfate direct radiative forcing in the Goddard Institute for Space Studies general circulation model. *Journal of Geophysical Research (Atmospheres)*, **104**, 23799-23822.

Krabill, W., *et al*., 1999: Rapid thinning of parts of the Southern Greenland Ice Sheet. *Science*, **283**, 1522-1524.

Krishnan, R., and V. Ramanathan, 2002: Evidence of surface cooling from absorbing aerosols. *Geophysical Research Letters*, **29**, doi:10.1029/2002GL014687.

Lean, J., 2000: Evolution of the Sun's spectral irradiance since the Maunder Minimum. *Geophysical Research Letters*, **27**, 2425-2428.

Lean, J., J. Beer, and R. Bradley, 1995: Reconstruction of solar irradiance since 1610: Implications for climate change. *Geophysical Research Letters*, **22**, 3195-3198.

Leroy, S.S., 1998: Detecting climate signals: Some Bayesian aspects. *Journal of Climate*, **11**, 640-651.

Levitus, S., J.I. Antonov, and T.P. Boyer, 2005: Warming of the world ocean, 1955-2003. *Geophysical Research Letters*, **32**, L02604, doi:10.1029/2004GL021592.

Levitus, S, *et al*., 2001: Anthropogenic warming of Earth's climate system. *Science*, **292**, 267-270.

Levitus, S., *et al*., 2000: Warming of the world ocean. *Science*, **287**, 2225-2229.

Lindzen, R.S., and C. Giannitsis, 1998: On the climatic implications of volcanic cooling. *Journal of Geophysical Research (Atmospheres)*, **103**, 5929-5941.

Manabe, S., and R.J. Stouffer, 1980: Sensitivity of a global climate model to an increase of CO_2 concentration in the atmosphere. *Journal of Geophysical Research (Atmospheres)*, **85**, 5529-5554.

Marshall, C.H., *et al*., 2004: The impact of anthropogenic land-cover change on the Florida Peninsula sea breezes and warm season sensible weather. *Monthly Weather Review*, **132**, 28-52.

Matthews, H.D., *et al*., 2004: Natural and anthropogenic climate change: incorporating historical land cover change, vegetation dynamics and the global carbon cycle. *Climate Dynamics*, **22**, 461-479.

Matthews, H.D., *et al*., 2003: Radiative forcing of climate by historical land cover change. *Geophysical Research Letters*, **30**, 1055, doi:10.1029/2002GL016098.

McAvaney, B.J., *et al*., 2001: Model evaluation. In: *Climate Change 2001: The Scientific Basis. Contribution of Working Group I to the Third Assessment Report of the Intergovernmental Panel on Climate Change* [Houghton, J.T., *et al*., (eds.)]. Cambridge University Press, Cambridge, United Kingdom and New York, NY, USA, 881 pp.

Mears, C.A., and F.W. Wentz, 2005: The effect of diurnal correction on satellite-derived lower tropospheric temperature. *Science*, **309**, 1548-1551.

Mears, C.A., M.C. Schabel, and F.W. Wentz, 2003: A reanalysis of the MSU channel 2 tropospheric temperature record. *Journal of Climate*, **16**, 3650-3664.

Meehl, G.A., *et al*., 2005: Climate change in the 20th and 21st centuries and climate change commitment in the CCSM3. *Journal of Climate* (in press).

Meehl, G.A., *et al*., 2000: The Coupled Model Intercomparison Project (CMIP). *Bulletin of the American Meteorological Society*, **81**, 313-318.

Meehl, G.A., 1984: Modeling the Earth's climate. *Climatic Change*, **6**, 259-286.

Menon, S., *et al*., 2002: Climate effects of black carbon aerosols in China and India. *Science*, **297**, 2250-2253.

Michaels, P.J., and P.C. Knappenberger, 2000: Natural signals in the MSU lower tropospheric temperature record. *Geophysical Research Letters*, **27**, 2905-2908.

Michaels, P.J., and P.C. and Knappenberger, 1996: Human effect on global climate? *Nature*, **384**, 523-524.

Min, S.-K., A. Hense, and W.-T. Kwon, 2005: Regional-scale climate change detection using a Bayesian detection method. *Geophysical Research Letters*, **32**, L03706, doi:10.1029/2004GL021028.

Minschwaner, K., *et al*., 1998: Infrared radiative forcing and atmospheric lifetimes of trace species based on observations from UARS. *Journal of Geophysical Research (Atmospheres)*, **103**, 23243-23253.

Mitchell, J.F.B., *et al*., 2001: Detection of climate change and attribution of causes. In: *Climate Change 2001: The Scientific Basis. Contribution of Working Group I to the Third Assessment Report of the Intergovernmental Panel on Climate Change* [Houghton, J.T., *et al*., (eds.)]. Cambridge University Press, Cambridge, United Kingdom and New York, NY, USA, 881 pp.

Murphy, J.M., *et al*., 2004: Quantification of modeling uncertainties in a large ensemble of climate simulations. *Nature*, **430**, 768-772.

Myhre, G., and A. Myhre, 2003: Uncertainties in radiative forcing due to surface albedo changes caused by land use changes. *Journal of Climate*, **16**, 1511-1524.

National Research Council, 2005: *Radiative Forcing of Climate Change: expanding the Concept and Addressing Uncertainties*. Board on Atmospheric Sciences and Climate, National Academy Press, Washington D.C., 168 pp.

National Research Council, 2000: *Reconciling Observations of Global Temperature Change*. Board on Atmospheric Sciences and Climate, National Academy Press, Washington D.C., 85 pp.

Nicholls, N., *et al*., 1996: Observed climate variability and change. In: *Climate Change 1995: The Science of Climate Change. Contribution of Working Group I to the Second Assessment Report of the Intergovernmental Panel on Climate Change* [Houghton, J.T., *et al*., (eds.)]. Cambridge University Press, Cambridge, United Kingdom and New York, NY, USA, 572 pp.

North, G.R., and M.J. Stevens, 1998: Detecting climate signals in the surface temperature record. *Journal of Climate*, **11**, 563-577.

North, G.R., *et al*., 1995: Detection of forced climate signals. Part I: Filter theory. *Journal of Climate*, **8**, 401-408.

Oleson, K.W., *et al*., 2004: Effect of land use change on North American climate: impact of surface datasets and model biogeophysics. *Climate Dynamics*, **23**, 117-132.

Pan, Y.H., and A.H. Oort, 1983: Global climate variations connected with sea surface temperature anomalies in the eastern equatorial Pacific Ocean for the 1958-73 period. *Monthly Weather Review*, **111**, 1244-1258.

1692 Paul, F., *et al*., 2004: Rapid disintegration of Alpine glaciers observed with satellite data.
1693 *Geophysical Research Letters*, **31**, L21402, doi:10.1029/2004GL020816.
1694
1695 Pawson, S., K. Labitzke, and S. Leder, 1998: Stepwise changes in stratospheric temperature.
1696 *Geophysical Research Letters*, **25**, 2157-2160.
1697
1698 Penner, J.E., *et al*., 2005: Effect of black carbon on mid-troposphere and surface temperature
1699 trends. In: *Integrated Assessment of Human Induced Climate Change*. [Schlesinger, M.E.
1700 (ed.)]. Cambridge University Press, Cambridge (in press).
1701
1702 Penner, J.E., S.Y. Zhang, and C.C. Chuang, 2003: Soot and smoke aerosol may not warm climate.
1703 *Journal of Geophysical Research (Atmospheres)*, **108**, 4657, doi:10.1029/2003JD003409.
1704
1705 Penner, J.E., *et al*., 2001: Aerosols, their direct and indirect effects. In: *Climate Change 2001: The*
1706 *Scientific Basis. Contribution of Working Group I to the Third Assessment Report of the*
1707 *Intergovernmental Panel on Climate Change* [Houghton, J.T., *et al*., (eds.)]. Cambridge
1708 University Press, Cambridge, United Kingdom and New York, NY, USA, 881 pp.
1709
1710 Pielke Sr., R.A., 2004: Assessing "global warming" with surface heat content. *EOS*, **85**, 210-211.
1711
1712 Pielke Sr., R.A., and T.N. Chase, 2004: Comment on "Contributions of anthropogenic and natural
1713 forcing to recent tropopause height changes". *Science*, **303**, 1771c.
1714
1715 Pielke Sr., R.A., 2003: Heat storage within the Earth system. *Bulletin of the American*
1716 *Meteorological Society*, **84**, 331-335.
1717
1718 Pierce, D.W., *et al*., 2005: Anthropogenic warming of the oceans: Observations and model results.
1719 *Journal of Climate* (in press).
1720
1721 Pitman, A.J., *et al*., 2004: Impact of land cover change on the climate of southwest Western
1722 Australia. *Journal of Geophysical Research (Atmospheres)*, **109**,
1723 doi:10.1029/2003JD004347.
1724
1725 Ramachandran, S., *et al*., 2000: Radiative impact of the Mount Pinatubo volcanic eruption: Lower
1726 stratospheric response. *Journal of Geophysical Research (Atmospheres)*, **105**, 24409-24429.
1727
1728 Ramanathan, V., *et al*., 2001: The Indian Ocean experiment: An integrated analysis of the climate
1729 forcing and effects of the great Indo-Asian haze. *Journal of Geophysical Research*
1730 *(Atmospheres)*, **106**, 28371-28398.
1731
1732 Ramankutty, N., and J.A. Foley, 1999: Estimating historical changes in global land cover:
1733 croplands from 1700 to 1992. *Global Biogeochemical Cycles*, **13**, 997-1027.
1734
1735 Ramaswamy, V., *et al*., 2006: Anthropogenic and natural influences in the evolution of lower
1736 stratospheric cooling. *Science* (in preparation).
1737

1738 Ramaswamy, V., *et al*., 2001a: Stratospheric temperature trends: observations and model
1739 simulations. *Reviews of Geophysics*, **39**, 71-122.
1740
1741 Ramaswamy, V., *et al*., 2001b: Radiative forcing of climate change. In: *Climate Change 2001: The*
1742 *Scientific Basis. Contribution of Working Group I to the Third Assessment Report of the*
1743 *Intergovernmental Panel on Climate Change* [Houghton, J.T., *et al*., (eds.)]. Cambridge
1744 University Press, Cambridge, United Kingdom and New York, NY, USA, 881 pp.
1745
1746 Ramaswamy, V., M.D. Schwarzkopf and W.J. Randel, 1996: Fingerprint of ozone depletion in the
1747 spatial and temporal pattern of recent lower-stratospheric cooling. *Nature*, **382**, 616-618.
1748
1749 Randel, W.J., and F. Wu, 2005: Biases in stratospheric temperature trends derived from historical
1750 radiosonde data. *Journal of Climate* (in press).
1751
1752 Randel, W.J., F. Wu, and D.J. Gaffen, 2000: Interannual variability of the tropical tropopause
1753 derived from radiosonde data and NCEP reanalyses. *Journal of Geophysical Research*
1754 *(Atmospheres)*, **105**, 15509-15523.
1755
1756 Randel, W.J., and F. Wu, 1999: Cooling of the Arctic and Antarctic polar stratosphere due to ozone
1757 depletion. *Journal of Climate*, **12**, 1467-1479.
1758
1759 Reichert, B.K., R. Schnur, and L. Bengtsson, 2002: Global ocean warming tied to anthropogenic
1760 forcing. *Geophysical Research Letters*, **29**, doi:10.1029/2001GL013954.
1761
1762 Rignot, E., and R.H. Thomas, 2002: Mass balance of polar ice sheets. *Science*, **297**, 1502-1506.
1763
1764 Robock, A., 2005: Using the Mount Pinatubo volcanic eruption to determine climate sensitivity:
1765 Comments on "Climate forcing by the volcanic eruption of Mount Pinatubo" by David H.
1766 Douglass and Robert S. Knox. *Geophysical Research Letters* (in press).
1767
1768 Robock, A., and C. Oppenheimer, 2003: *Volcanism and the Earth's Atmosphere*. AGU
1769 Geophysical Monograph Series, **139**, Washington D.C. American Geophysical Union, 360
1770 pp.
1771
1772 Robock, A., 2000: Volcanic eruptions and climate. *Reviews of Geophysics*, **38**, 191-219.
1773
1774 Rodwell, M.J., D.P. Rowell, and C.K. Folland, 1999: Oceanic forcing of the wintertime North
1775 Atlantic Oscillation and European climate. *Nature*, **398**, 320-323.
1776
1777 Santer, B.D., *et al*., 2005: Amplification of surface temperature trends and variability in the tropical
1778 atmosphere. *Science*, **309**, 1551-1556.
1779
1780 Santer, B.D., *et al*., 2004: Identification of anthropogenic climate change using a second-generation
1781 reanalysis. *Journal of Geophysical Research (Atmospheres)*, **109**,
1782 doi:10.1029/2004JD005075.
1783

Santer, B.D., *et al*., 2003a: Contributions of anthropogenic and natural forcing to recent tropopause height changes. *Science*, **301**, 479-483.

Santer, B.D., *et al*., 2003b: Influence of satellite data uncertainties on the detection of externally-forced climate change. *Science*, **300**, 1280-1284.

Santer, B.D., *et al*., 2001: Accounting for the effects of volcanoes and ENSO in comparisons of modeled and observed temperature trends. *Journal of Geophysical Research (Atmospheres)*, **106**, 28033-28059.

Santer, B.D., *et al*., 2000: Interpreting differential temperature trends at the surface and in the lower troposphere. *Science*, **287**, 1227-1232.

Santer, B.D., *et al*., 1999: Uncertainties in observationally-based estimates of temperature change in the free atmosphere. *Journal of Geophysical Research (Atmospheres)*, **104**, 6305-6333.

Santer, B.D., *et al*., 1996a: A search for human influences on the thermal structure of the atmosphere. *Nature*, **382**, 39-46.

Santer, B.D. *et al*., 1996b: Human effect on global climate? *Nature*, **384**, 522-524.

Satheesh, S.K., and V. Ramanathan, 2000: Large differences in tropical aerosol forcing at the top of the atmosphere and Earth's surface. *Nature*, **405**, 60-63.

Sato, M., *et al*., 1993: Stratospheric aerosol optical depths, 1850-1990: *Journal of Geophysical Research (Atmospheres)*, **98**, 22987-22994.

Seidel, D.J., *et al*., 2004: Uncertainty in signals of large-scale climate variations in radiosonde and satellite upper-air temperature datasets. *Journal of Climate*, **17**, 2225-2240.

Seidel, D.J., and J.R. Lanzante, 2004: An assessment of three alternatives to linear trends for characterizing global atmospheric temperature changes. *Journal of Geophysical Research (Atmospheres)*, **109**, doi: 10.1029/2003JD004414.

Seidel, D.J., R.J. Ross, J.K. Angell, and G.C. Reid, 2001: Climatological characteristics of the tropical tropopause as revealed by radiosondes. *Journal of Geophysical Research (Atmospheres)*, **106**, 7857-7878.

Sexton, D.M.H., *et al*., 2001: Detection of anthropogenic climate change using an atmospheric GCM. *Climate Dynamics*, **17**, 669-685.

Sherwood, S.C., J. Lanzante, and C. Meyer, 2005: Radiosonde daytime biases and late 20th century warming. *Science*, **309**, 1556-1559.

1828 Shindell, D.T., G. Fulavegi, and N. Bell, 2003: Preindustrial-to-present-day radiative forcing by
1829 tropospheric ozone from improved simulations with the GISS chemistry-climate GCM.
1830 *Atm. Chem. Phys*., **3**, 1675-1702.
1831
1832 Shine, K.P., *et al*., 2003: A comparison of model-simulated trends in stratospheric temperatures.
1833 *Quarterly Journal of the Royal Meteorological Society*, **129**, 1565-1588.
1834
1835 Smith, S.J., H. Pitcher, and T.M.L. Wigley, 2005: Future sulfur dioxide emissions. *Climatic*
1836 *Change*, **73**, 267-318.
1837
1838 Smith, S.J., H. Pitcher, and T.M.L. Wigley, 2001: Global and regional anthropogenic sulfur dioxide
1839 emissions. *Global and Planetary Change*, **29**, 99-119.
1840
1841 Soden, B.J., *et al*., 2002: Global cooling after the eruption of Mt. Pinatubo: A test of climate
1842 feedback by water vapor. *Science*, **296**, 727-730.
1843
1844 Soden, B.J., 2000: the sensitivity of the tropical hydrological cycle to ENSO. *Journal of Climate*,
1845 **13**, 538-549.
1846
1847 Stainforth, D.A., *et al*., 2005: Uncertainties in predictions of the climate response to rising levels of
1848 greenhouse gases. *Nature*, **433**, 403-406.
1849
1850 Stott, P.A., *et al*., 2005: Robustness of estimates of greenhouse attribution and observationally
1851 constrained predictions of global warming. *Journal of Climate* (accepted).
1852
1853 Stott, P.A., D.A. Stone, and M.R. Allen, 2004: Human contribution to the European heatwave of
1854 2003. *Nature*, **423**, 61-614.
1855
1856 Stott, P.A., 2003: Attribution of regional-scale temperature changes to anthropogenic and natural
1857 causes. *Geophysical Research Letters*, **30**, doi: 10.1029/2003GL017324.
1858
1859 Stott, P.A., *et al*., 2000: External control of 20th century temperature by natural and anthropogenic
1860 forcings. *Science*, **290**, 2133-2137.
1861
1862 Stott, P.A., and S.F.B. Tett, 1998: Scale-dependent detection of climate change. *Journal of*
1863 *Climate*, **11**, 3282-3294.
1864
1865 Sun, S., and J.E. Hansen, 2003: Climate simulations for 1951-2050 with a coupled atmosphere-
1866 ocean model. *Journal of Geophysical Research (Atmospheres)*, **16**, 2807-2826.
1867
1868 Tett, S.F.B., and P.W. Thorne, 2004: Comment on tropospheric temperature series from satellites.
1869 *Nature*, doi: 10.1038/nature03208.
1870
1871 Tett, S.F.B., *et al*., 2002: Estimation of natural and anthropogenic contributions to twentieth
1872 century temperature change. *Journal of Geophysical Research (Atmospheres)*, **107**,
1873 doi:10.1029/2000JD000028.

Tett, S.F.B., *et al*., 1999: Causes of twentieth-century temperature change near the Earth's surface. *Nature*, **399**, 569-572.

Tett, S.F.B., *et al*., 1996: Human influence on the atmospheric vertical temperature structure: Detection and observations. *Science*, **274**, 1170-1173.

Thorne, P.W., *et al*., 2005: Revisiting radiosonde upper-air temperatures from 1958 to 2002. *Journal of Geophysical Research (Atmospheres)* (in press).

Thorne, P.W., *et al*., 2003: Probable causes of late twentieth century tropospheric temperature trends. *Climate Dynamics*, **21**, 573-591.

Thorne, P.W., *et al*., 2002: Assessing the robustness of zonal mean climate change detection. *Geophysical Research Letters*, **29**, doi: 10.1029/2002GL015717.

Tie, X., *et al*., 2005: Assessment of the global impact of aerosols on tropospheric oxidants. *Journal of Geophysical Research (Atmospheres)* (in press).

Trenberth, K.E., J. Fasullo, and L. Smith, 2005: Trends and variability in column-integrated atmospheric water vapor. *Climate Dynamics*, doi:10.1007/s00382-005-0017-4.

Trenberth, K.E., and L. Smith, 2005: The mass of the atmosphere: A constraint on global analyses. *Journal of Climate*, **18**, 860-875.

Trenberth, K.E., and T.J. Hoar, 1996: The 1990-1995 El Niño-Southern Oscillation event: longest on record. *Geophysical Research Letters*, **23**, 57-60.

Trenberth, K.E., 1992: *Climate System Modeling*. Cambridge University Press, Cambridge, 788 pp.

Wallace, J.M., Y. Zhang, and J.A. Renwick, 1995: Dynamic contribution to hemispheric mean temperature trends. *Science*, **270**, 780-783.

Washington, W.M., *et al*., 2000: Parallel Climate Model (PCM) control and transient simulations. *Climate Dynamics*, **16**, 755-774.

Weber, G.R., 1996: Human effect on global climate? *Nature*, **384**, 524-525.

Wehner, M.F., 2000: A method to aid in the determination of the sampling size of AGCM ensemble simulations. *Climate Dynamics*, **16**, 321-331.

Wentz, F.J., and M. Schabel, 2000: Precise climate monitoring using complementary satellite data sets. *Nature*, **403**, 414-416.

Wielicki, B.A., *et al*., 2002: Evidence for large decadal variability in the tropical mean radiative energy budget. *Science*, **295**, 841-844.

Wigley, T.M.L., *et al*., 2005a: The effect of climate sensitivity on the response to volcanic forcing. *Journal of Geophysical Research (Atmospheres)*, **110**, D09107, doi:10.1029/2004JD005557.

Wigley, T.M.L., *et al*., 2005b: Using the Mount Pinatubo volcanic eruption to determine climate sensitivity: Comments on "Climate forcing by the volcanic eruption of Mount Pinatubo", by David H. Douglass and Robert S. Knox. *Geophysical Research Letters* (in press).

Wigley, T.M.L., 2000: ENSO, volcanoes, and record-breaking temperatures. *Geophysical Research Letters*, **27**, 4101-4104.

Willis, J.K., D. Roemmich, and B. Cornuelle, 2004: Interannual variability in upper-ocean heat content, temperature, and thermosteric expansion on global scales. *Journal of Geophysical Research*, **109**, C12036, doi:10.1029/2003JC002260..

Yulaeva, E., and J.M. Wallace, 1994: The signature of ENSO in global temperature and precipitation fields derived from the microwave sounding unit. *Journal of Climate*, **7**, 1719-1736.

Zwiers, F.W., and X. Zhang, 2003: Towards regional-scale climate change detection. *Journal of Climate*, **16**, 793-797.